AGU PUBLICATIONS

JGR

Journal of Geophysical Research: Atmospheres

RESEARCH ARTICLE
10.1002/2016JD025683

Key Points:
- WRF outputs provide a noticeable improvement over ERA-Interim for many regions in Spain, greater for SPI than for SPEI
- The improvement offered by WRF in simulating drought indices is greater at longer time scales
- Dynamical downscaled fields provide benefits to detect and analyze wet and dry periods over a region with high precipitation variability

Correspondence to:
M. J. Esteban-Parra,
esteban@ugr.es

Citation:
García-Valdecasas Ojeda, M., S. R. Gámiz-Fortis, Y. Castro-Díez, and M. J. Esteban-Parra (2017), Evaluation of WRF capability to detect dry and wet periods in Spain using drought indices, *J. Geophys. Res. Atmos.*, *122*, 1569–1594, doi:10.1002/2016JD025683.

Received 21 JUL 2016
Accepted 22 JAN 2017
Accepted article online 25 JAN 2017
Published online 7 FEB 2017

©2017. The Authors.
This is an open access article under the terms of the Creative Commons Attribution-NonCommercial-NoDerivs License, which permits use and distribution in any medium, provided the original work is properly cited, the use is non-commercial and no modifications or adaptations are made.

Evaluation of WRF capability to detect dry and wet periods in Spain using drought indices

Matilde García-Valdecasas Ojeda[1], Sonia R. Gámiz-Fortis[1], Yolanda Castro-Díez[1], and María Jesús Esteban-Parra[1]

[1]Departamento de Física Aplicada, Facultad de Ciencias, Universidad de Granada, Granada, Spain

Abstract The Weather Research and Forecasting (WRF) model has been used to show the benefits provided by downscaled fields to detect and analyze wet and dry periods over a region with high precipitation variability such as Spain. We have analyzed the spatiotemporal behavior of two widely used drought indices: the Standardized Precipitation Index (SPI) and the Standardized Precipitation Evapotranspiration Index (SPEI), computed at 3 and 12 month time scales, which provide important information in an agricultural and water-resource context. These two indices were computed from WRF outputs and compared with those calculated from observational (monthly precipitation and temperature databases of Spain, MOPREDAS and MOTEDAS) and from the European Centre for Medium-Range Weather Forecasts Interim Re-Analysis (ERA-Interim) data sets. This evaluation was made by using a regional scale and a multistep regionalization method and by comparison of individual grid points. In general, results indicate that the drought indices obtained by using WRF outputs provide a noticeable improvement regarding those computed by using ERA-Interim, higher at longer time scales. Although results show no significant differences between drought indices analyzed, the improvement offered by WRF is greater for SPI than for SPEI. In terms of averaged duration, magnitude, and severity of drought, the benefits provided by WRF are not so evident, presenting better agreement with the observational data at 12 month time scale, being clearer for the intensity. These findings evidence the benefit of using WRF climate fields to monitor, analyze, and detect drought events, being a valuable source of knowledge for a suitable decision making, especially for water-resource management.

1. Introduction

The increase in drought episodes is one of the most threatening natural hazards related to climate change [*Sheffield and Wood*, 2008]. The drought phenomenon, which is characterized mainly by being a period with scarce precipitation, causes serious economic, social, and environmental impact with tremendous losses, especially in vulnerable areas such as the Mediterranean region [*Christensen et al.*, 2007; *Lindner et al.*, 2010]. In recent years, the Mediterranean region has undergone severe drought events, a clear instance being the drought of 2005 [*Kennedy et al.*, 2006], which was particularly strong in Spain and Portugal [*García-Herrera et al.*, 2007]. The hazard of an increase in the frequency and severity of these extreme events due to climate change in regions such as the Mediterranean [*Blenkinsop and Fowler*, 2007; *Sánchez et al.*, 2011] makes it necessary to evaluate the future potential impact related to droughts in order to design mitigation and adaptation strategies and thereby reduce their effects on the population.

To define drought phenomena, different indices have been developed in recent years, which allow the quantification of wet and dry periods. No single index performs better than others, so for an adequate election of this, it is important to consider several aspects such as the ability to capture the spatiotemporal characteristics of droughts in the study region [*PaiMazumder and Done*, 2014] and the main features of the drought index (e.g., calculation procedure, input variables, advantages, and weakness). The Standardized Precipitation Index (SPI) [*McKee et al.*, 1993] is recommended by the World Meteorological Organization, due to its simplicity, robustness, easy interpretation, and especially for its multiscalar character. This last characteristic is essential to detect different drought types and their impacts [*Guttman*, 1998; *Vicente-Serrano et al.*, 2010; *Beguería et al.*, 2014]. Additionally, the SPI has the advantage of being comparable across regions with markedly different climates, thus being very useful to detect, monitor, and analyze droughts in different regions of the world. Nevertheless, the SPI only uses precipitation data to detect drought events. By contrast, the Palmer Drought Severity Index (PDSI) [*Palmer*, 1965] is one of the most widely applied drought indices [*Mishra and Singh*, 2010], which is mainly used to monitor long-term droughts. The PDSI considers the effects of the temperature throughout reference evapotranspiration, so it is more suitable than the SPI in a context of

21698996, 2017, 3, Downloaded from https://agupubs.onlinelibrary.wiley.com/doi/10.1002/2016JD025683 by Readcube (Labtiva Inc.), Wiley Online Library on [27/01/2024]. See the Terms and Conditions (https://onlinelibrary.wiley.com/terms-and-conditions) on Wiley Online Library for rules of use; OA articles are governed by the applicable Creative Commons License

global warming. Nonetheless, the PDSI is spatially incomparable, complicated to calculate and to understand, and temporally invariable (i.e., it has no multiscalar properties) [*Guttman*, 1998]. Another index, the Standardized Precipitation Evapotranspiration Index (SPEI) [*Vicente-Serrano et al.*, 2010], is a relatively new index which has been already used in a large number of climatological, hydrological, and ecological studies [*Yu et al.*, 2014; *Meque and Abiodun*, 2015; *Kim et al.*, 2016; *Wang et al.*, 2016] because it combines the benefit of using the reference evapotranspiration, like the PDSI, with the simplicity, robustness, and the multiscalar properties of the SPI [*Vicente-Serrano et al.*, 2010, 2011c, 2014b].

The study of future drought events requires the use of global climate models (GCMs) [*Burke et al.*, 2006; *Wang*, 2005]. However, due to their coarse resolution, GCMs are unable to capture the regional behavior of the droughts in areas with high precipitation variability such as Mediterranean region [*Vicente-Serrano et al.*, 2004]. This problem could be solved by the application of regional climate models (RCMs) to capture the different processes related to drought episodes at a finer scale. Nevertheless, RCM simulations also present difficulties because of the sources of uncertainty caused by different aspects such as the internal variability of the regional model, the different possibilities of the configuration (e.g., parameterization schemes or dynamic parameters), the nesting procedure used, and also factors related to errors inherited from the initial and boundary conditions [*PaiMazumder and Done*, 2014]. Therefore, prior to the use of an RCM for climate-change studies, it is essential to evaluate the ability of the RCM to capture regional climate characteristics in order to analyze whether the RCM provides an improvement over the driving data. In this context, *Argüeso et al.* [2012a] demonstrated the ability of the Weather Research and Forecasting (WRF) model to capture the frequency and the main spatial patterns of rainfall in Spain, which is the most important variable related to drought events. Regarding temperature, which is another key variable for droughts, *Gonçalves et al.* [2014] have also shown the improvements provided by the dynamical downscaling based on WRF in terms of this variable in this topographically complex region.

For other areas, drought-simulation studies have already been conducted, and the benefit of using RCMs for this has been confirmed. *PaiMazumder and Done* [2014] assessed the ability of an ensemble of Canadian Regional Climate Model to simulate long-term drought episodes over different watersheds located in Canada. This evaluation was performed in terms of severity, frequency, and duration of droughts based on the self-calibrated Palmer Drought Severity Index (PDSI) and the Drought Severity Index (DSI). The results suggested that the models have problems in capturing these observed drought characteristics. *Maule et al.* [2013] evaluated the precipitation deficit of a set of simulations from the project ENSEMBLES over Europe in terms of two drought indices, the SPI and the PDSI. They found that, in general, the models suitably capture the most severe dry episodes. However, they also observed that, in geographically complex regions, several models perform poorly when the precipitation is very scarce. *Bowden et al.* [2016] showed the added value provided by downscaled fields in order to detect drought events by using the SPI index, at different time scales over the contiguous United States. That study revealed that the improvement provided by WRF with respect to the driving data is higher at longer time scales. *Barrera-Escoda et al.* [2014] also assessed the ability of the WRF model to reproduce extreme values of precipitation and temperature for a period between 1971 and 2000 over the northwestern Mediterranean Basin (covering only the northwestern part of Spain and southern France) by using 12 month SPEI. In this way, they determined the occurrence of dry and wet periods, finding good agreement with respect to observations in the temporal series of SPEI with a high temporal correlation ($r = 0.61$).

Based on the above, the main goal of this study is to ascertain the improvement provided by the WRF model as RCM to detect dry and wet periods in terms of drought indices for Spain, a topographically complex area. First, this study evaluates the method proposed by *Bowden et al.* [2016] over Spain in terms of drought indices. This method is based on the comparison between the temporal series of drought indices computed from the WRF outputs and driving data regarding those obtained from the observational data set, in terms of different parameters such as the temporal correlation coefficients or other metrics. For that, two drought indices have been used: an index only based on precipitation data, the SPI, and another one that also takes into account temperature data, the SPEI. In this study, the selection of drought indices was based on two main aspects: the spatial comparability and the multiscalar properties of these indices, which allows analyzing properly agricultural and hydrological droughts. Furthermore, the only difference between the two drought indices is the consideration of the temperature, so the comparison between them enables an appropriate analysis of the simulated temperature effects on drought events. Authors such as *Vicente-Serrano et al.* [2014b] proved the

21698996, 2017, 3, Downloaded from https://agupubs.onlinelibrary.wiley.com/doi/10.1002/2016JD025683 by Readcube (Labtiva Inc.), Wiley Online Library on [27/01/2024]. See the Terms and Conditions (https://onlinelibrary.wiley.com/terms-and-conditions) on Wiley Online Library for rules of use; OA articles are governed by the applicable Creative Commons License

suitability of using the SPEI and SPI in order to detect drought phenomena in Spain. Additionally, in this study, the WRF's capability to simulate important drought characteristics such as the magnitude, the severity, and the duration of drought has been also evaluated. Comparing results in terms of drought characteristics, for both indices at different time scales, improves the understanding about the WRF behavior to detect these extreme events. We describe the WRF setup applied, the data, and the statistical drought-evaluation method used to prove the added value of the WRF model in section 2. Section 3 presents the results by using a regional approach, with comparisons directly to grip points. Finally, in section 4, we conclude and discuss the results found.

2. Methods

2.1. The WRF Model Configuration

The Weather Research and Forecasting model with the Advanced Research WRF dynamic core, WRF-ARW [*Skamarock et al.*, 2008] version 3.6.1, has been used to perform regional climate simulations. WRF is a mesoscale numerical weather-prediction system that has been widely applied as regional climate model (RCM) to simulate present and future climate in terms of different variables [*Boulard et al.*, 2016; *Kala et al.*, 2015; *Argüeso et al.*, 2012a, 2012b].

In the present study, the model configuration (Figure 1a) consists of two one-way nested domains: the coarser domain (d01), which corresponds to the European Coordinated Regional Climate Downscaling Experiment (EURO-CORDEX) region [*Giorgi et al.*, 2009; *Jacob et al.*, 2014], encompassing the entire European Union on a 120×130 rotated latitude-longitude grid with a horizontal resolution of 0.44° (about 50 km), and the nested domain (d02), with a 221×221 grid centered over the Iberian Peninsula at a horizontal resolution of 0.088° (~10 km). In the vertical, both domains were composed of 41 levels with the topset to 10 hPa. The study period spanned from January 1979 until November 2010, which was divided into three 10 year continuous runs, in order to optimize the computational resources [*Pan et al.*, 1999]. For each 10 year simulation, the first 11 months were considered as the spin-up of the model in order to avoid imbalances between external forcing and internal dynamics [*Hamdi et al.*, 2014]. As this study is focused on high-resolution climate fields, only the nested domain solutions were assessed.

WRF has been driven by the ERA-Interim reanalysis data set [*Berrisford et al.*, 2011; *Dee et al.*, 2011] (hereafter referred as ERA) every 6 h at a 0.75° horizontal resolution and 37 vertical pressure levels (from 1000 to 1 hPa). To avoid inconsistencies along boundaries, we applied a spectral nudging (SN) technique [*Waldron et al.*, 1996; *von Storch et al.*, 2000; *Miguez-Macho et al.*, 2004]. All simulations were nudged with wave numbers of 10 and 11 in the *x* and *y* directions, respectively, which means to adjust only waves above 600 km and used only in the coarser domain and above the planetary boundary layer (PBL) in order to allow the RCM to perform its own internal dynamic in the finer resolution domain [*Pérez et al.*, 2014; *Heikkilä et al.*, 2011]. The SN was applied for winds, temperature, and geopotential height. However, this SN technique was not applied for humidity, avoiding errors associated to the competition with the convective scheme [*Argüeso et al.*, 2012a].

The parameterization schemes were chosen in accordance with a previous test performed in this region [*García-Valdecasas-Ojeda et al.*, 2015], which suggested that a reliable set of physics schemes includes asymmetric convective model version 2 [*Pleim*, 2007] for the PBL, Betts-Miller-Janjic [*Betts and Miller*, 1986; *Janjic*, 1990, 1994] for cumulus, and the WRF single-moment three-class schemes [*Hong et al.*, 2004] for microphysics. On the other hand, the Noah land-surface model [*Chen and Dudhia*, 2001] scheme was chosen as a land-surface model, since it is a widely accepted scheme in climate simulations, and the Community Atmosphere Model 3.0 [*Collins et al.*, 2004] was used for both long-wave and short-wave radiation schemes with the aim of updating the atmospheric concentrations of greenhouse gases. The suitability of this set of physic schemes over Spain was corroborated by authors such as *Argüeso et al.* [2011], who carried out a WRF sensitivity study in a similar region and later confirmed that it was adequate to perform high-resolution projections of mean and extreme precipitation over Spain [*Argüeso et al.*, 2012b].

The daily accumulated precipitation was stored at 0700 UTC every day in order to compare the WRF outputs with the observations. Surface-temperature extremes (maximum and minimum temperatures) were determined by using the CLimate WRF module [*Fita et al.*, 2010] and stored daily.

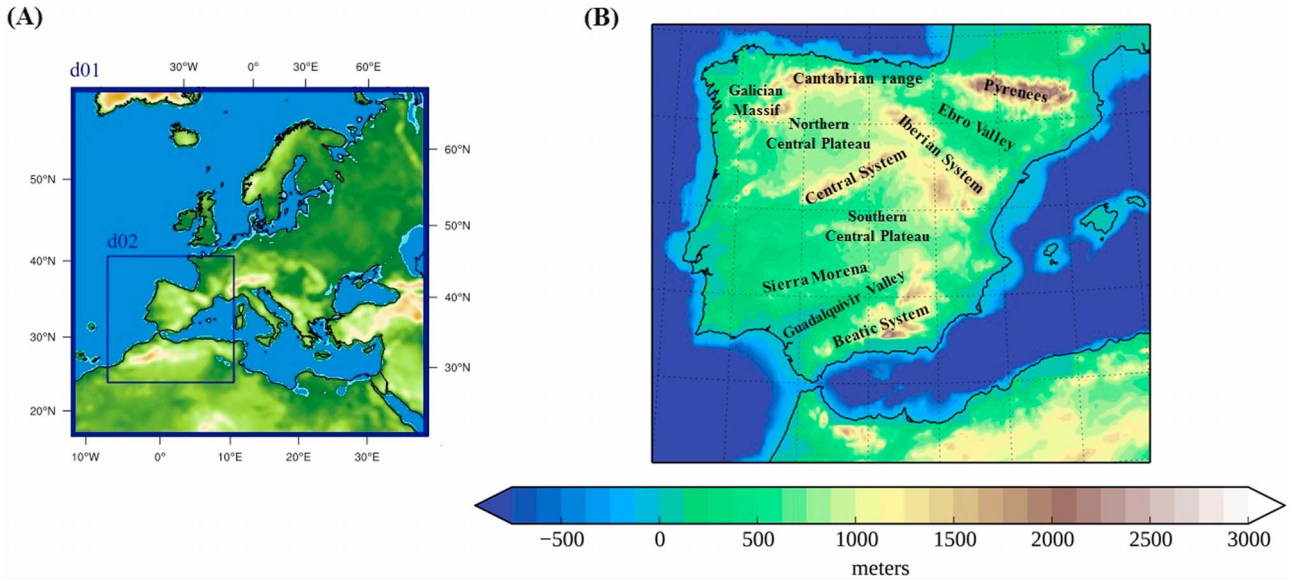

Figure 1. (a) Domain of the study: the 0.44 EURO-CORDEX domain (d01) as coarser domain and an inner domain (d02) centered over the Iberian Peninsula with a horizontal resolution of 0.088°. (b) Main topographical features of Spain.

2.2. Drought Indices: The SPI and the SPEI

This study evaluates the capability of WRF to simulate wet and dry periods by using two different drought indices, the SPI and the SPEI. Both indices have the same calculation procedure with the difference that SPEI uses a "climatic water balance" instead of precipitation data, that is, the difference between accumulated precipitation and reference evapotranspiration (ET_0). Therefore, a critical step to determine the SPEI is to choose a suitable method to compute the ET_0. To calculate the ET_0, we chose the modified Hargreaves equation (HG-PP) [*Droogers and Allen*, 2002]. The HG-PP corrects the ET_0 calculated from the Hargreaves equation based on the hypothesis that the monthly accumulated precipitation value can change the humidity levels [*Vicente-Serrano et al.*, 2014a]. Using the HG-PP, we obtain similar results to those provided of the Penman-Monteith equation [*Allen et al.*, 1998], which is the method adopted and recommended by the Food and Agriculture Organization to approximate this parameter, with the advantage that it requires only precipitation and maximum and minimum temperatures [*Beguería et al.*, 2014]. Furthermore, the HG-PP model provides good agreement in order to compute the ET_0 in Spain [*Vicente-Serrano et al.*, 2014b].

In this study, the SPEI R package [*Beguería and Vicente-Serrano*, 2013] was used to compute the SPEI and SPI indices. The SPEI R package applies the method provided by *Vicente-Serrano et al.* [2010], which is based on the fit to a statistical distribution of the aggregated values of precipitation and climate water balance for SPI and SPEI, respectively, at different time scales. These original values are then transformed to a normal distribution that enables a comparison in space and time. Due to the response of different systems, such as the hydrological or agricultural system, the result depends on the time scales used. Thereby, we computed these indices at two different time scales: the 3 month time scale, which allows the study of episodes related to agricultural droughts since it is suitable to analyze variations in the soil moisture content available for vegetation [*Sims et al.*, 2002; *Santos et al.*, 2010], and the 12 month time scale in order to detect hydrological droughts and its effects in river streamflows and water resources [*Vicente-Serrano*, 2006]. Additionally, for comparative purposes, drought indices were fitted to a log-logistic probability distribution by using the maximum-likelihood method. This ensures that the differences between the two indices were related to the temperature effects and not to the probability distribution used [*Vicente-Serrano et al.*, 2011a].

2.3. Regionalization of Observational Drought Indices

Drought indices computed by using WRF output fields were compared against those from observational databases. For that, we used the gridded data set from monthly precipitation database of Spain (MOPREDAS) [*González-Hidalgo et al.*, 2011] for precipitation and monthly temperature database of Spain

21698996, 2017, 3, Downloaded from https://agupubs.onlinelibrary.wiley.com/doi/10.1002/2016JD025683 by Readcube (Labtiva Inc.), Wiley Online Library on [27/01/2024]. See the Terms and Conditions (https://onlinelibrary.wiley.com/terms-and-conditions) on Wiley Online Library for rules of use; OA articles are governed by the applicable Creative Commons License

21698996, 2017, 3, Downloaded from https://agupubs.onlinelibrary.wiley.com/doi/10.1002/2016JD025683 by Readcube (Labtiva Inc.), Wiley Online Library on [27/01/2024]. See the Terms and Conditions (https://onlinelibrary.wiley.com/terms-and-conditions) on Wiley Online Library for rules of use; OA articles are governed by the applicable Creative Commons License

(MOTEDAS) [*González-Hidalgo et al.*, 2015] for maximum and minimum temperatures (hereafter jointly referred to as mprmt). Both databases were developed by using quality-controlled series from the Spanish Meteorological Agency (Agencia Estatal de Meteorología) stations (2670 for precipitation and 1358 for temperature) providing a high-resolution monthly 0.1° regularly gridded data set that covers peninsular Spain for the period of 1950–2010.

To facilitate the comparison in terms of the spatiotemporal evolution of wet and dry periods, we grouped the observational gridded data by using a multistep regionalization procedure. For this reason, we employed a regionalization technique following the procedure suggested in *Argüeso et al.* [2011], the first step being the computation of the monthly observational SPEI series. In this way, the SPEI series were established for the entire period (1950–2010) at 3 and 12 month time scales. Then, a principal component analysis in *S* mode [*Wilks*, 2006] was applied to the SPEI anomalies by using the covariance matrix in order to reduce redundant information by retaining the principal modes of variability [*Fovell*, 1997]. The principal components retained were rotated, redistributing the explained variance and increasing the spatial coherence by using the Varimax [*Richman*, 1986] method. For this, the number of components that explained a minimum of about 80% of the temporal variability [*Russo et al.*, 2015] of the SPEI was selected. Rotated factor loadings were used to apply an agglomerative clustering analysis (CA) method so as to set the number of clusters and obtain the starting seeds. In this step, the square Euclidean distance was selected as a measurement of similarity and the average linkage algorithm as a method to group each object into a cluster. The optimal number of clusters was determined by using the pseudo *F* test [*Calinski and Harabasz*, 1974]. Finally, a nonhierarchical k-means CA was used in order to identify the most suitable regions because k-means algorithm checks each of the cluster members and reallocates the grid points according to the spatial coherence. Thus, a k-means CA was performed by using the same number of clusters and the spatial average of the SPEI series for each region indicated by the agglomerative CA as initial centroids.

2.4. Statistical Evaluation

To evaluate the capacity of WRF to detect dry and wet periods, the results of computing drought indices at regionalized scale and directly comparing grid points were analyzed. Thus, the drought indices from WRF outputs using ERA as the boundary conditions (hereafter jointly referred to as WRFERA) and from mprmt were computed. The ERA data set was also used for evaluating the added value that the dynamical downscaling offers with respect to the driving data. All indices were calculated for the period of 1 December 1979 to 30 November 2010, using the monthly average of maximum and minimum temperatures and accumulated precipitation. Because each database has a different horizontal resolution, the ERA and WRFERA data sets were previously regridded to an mprmt 0.1° regular grid by using a bilinear interpolation, in order to make the different drought indices comparable.

2.4.1. Regional Analysis

In a regional context, the SPEI and SPI series for each grid point were grouped by using the regions of reference obtained in the regionalization technique, and then, the temporal series for each region were established as the simple average of all grid points in this region. Thus, we quantify the benefit of using WRF output by comparing the temporal evolution of WRFERA and ERA series with respect to those computed with the observed data by using the temporal correlation coefficients. The difference between WRFERA and ERA correlation coefficients has been also used to quantify the benefit that provides the downscaled fields for both indices and time scales in all regions.

2.4.2. Local Analysis

To analyze the benefit gained by using downscaled fields in more detail, we also calculated different parameters directly by comparisons of grid point to grid point since the results obtained at regional scale by using averaged temporal evolution of drought indices could mask effects related to local droughts.

2.4.2.1. Local Evaluation of Dry and Wet Episodes Using Drought Indices

For the reason mentioned above, we calculated different statistics for SPEI and SPI series at the two different time scales. First, the root-mean-square errors (RMSEs) between WRFERA and mprmt as well as between ERA and mprmt over every grid points were calculated. Thus, we quantify the model ability to capture the temporal variability of droughts.

In terms of spatial variability, the procedure detailed in *Wang et al.* [2015] was applied, which is based on calculating the Pearson correlation coefficients at different spatial intervals along longitude and latitude. The spatial correlation coefficient is calculated by

$$r_{L,l,s_1,s_2} = \frac{\sum_{i=1}^{n}\left(x_{i,L,l} - \overline{x}_{L,l}\right)\left(x_{i,L+s_1,l+s_2} - \overline{x}_{L+s_1,l+s_2}\right)}{\sqrt{\sum_{i=1}^{n}\left(x_{i,L,l} - \overline{x}_{L,l}\right)^2}\sqrt{\sum_{i=1}^{n}\left(x_{i,L+s_1,l+s_2} - \overline{x}_{L+s_1,l+s_2}\right)^2}} \quad (1)$$

where x corresponds to drought index values for every i month with coordinates (L, l) in latitude and longitude, respectively, s_1 is the south-to-north interval, and s_2 is the west-to-east interval. Thereby, we have calculated spatial correlations from WRFERA, ERA, and mprmt by using a lag of 0.4°, and then, the added value is assessed by direct comparison of the differences between WRFERA-mprmt and ERA-mprmt. This analysis provides information of the spatial behavior of the WRF model, and therefore, the added value of using high-resolution fields to compute drought indices over topographically complex regions.

To quantify the added value provided by downscaling techniques by using a categorical point of view, the Critical Success Index (CSI) [*Kang et al.*, 2005] was also analyzed. The CSI measures whether the model is able to capture dry and wet episodes above a certain threshold. The CSI was calculated by following the procedure carried out by *Bowden et al.* [2016], who calculated the CSI for events with SPI above 1 and below −1, which are known as exceedances. The CSI is defined as

$$\mathrm{CSI}(\%) = \frac{\mathrm{TP}}{\mathrm{TP} + \mathrm{FP} + \mathrm{FN}} \times 100 \quad (2)$$

where TP are the exceedances given by ERA or WRFERA and corroborated by mprmt (true positives), FP are the ones found by using ERA and WRFERA that are not corroborated by mprmt (false positives), and FN are the noncaptured ERA and WRFERA exceedances that occurred (false negatives). As our goal is to determinate the WRF ability to characterize moderate-to-extreme wet and dry periods, the analysis was performed jointly for events with a drought index above 1 and below −1. The difference between the CSI calculated from WRFERA and ERA drought indices with respect to mprmt is another way to evaluate the added value provided by downscaled fields. To determine the statistical significance of the CSI difference, the two-proportion z-test [*Yang et al.*, 2015] was applied, which consists of a significance test whose null hypothesis supposes that there is no difference between the CSI based on modeled data and those calculated by using observations. This test was used at the 95% confidence level.

2.4.2.2. Local Evaluation of Drought Characteristics: Duration, Magnitude, and Severity

A study on the potential capacity of the WRF model to provide suitable predictions of future drought episodes was also performed by using different characteristics such as the duration, the magnitude, and the severity of individual drought events. Thus, we defined a dry episode when the values of the SPEI and SPI were below 0 [*Vicente-Serrano et al.*, 2011a]. Therefore, the duration, severity, and magnitude series of individual drought events can be computed, understanding the duration as number of consecutive months with negative index values, the severity as the maximum SPEI or SPI value of each episode, and the magnitude as the sum of the drought values for each episode.

We evaluated the ability of WRF and the driving data to capture drought characteristics by using the temporal average of the duration, severity, and magnitude for the entire study period, for both indices and time scales. The comparison between modeled and observed data was used to evaluate whether WRF outperforms the driving data in terms of mean values of drought characteristics.

The duration, magnitude, and severity series were obtained for every grid point. From these series we calculated their corresponding Perkins Skill Score (SS) [*Perkins et al.*, 2007]. Perkins SS measures the similarity between observed and simulated distributions, using for that the common area between their probability density functions (PDFs). The formal expression of this skill score is

$$SS_{\mathrm{score}} = \sum_{1}^{n} \min(Z_m, Z_0) \quad (3)$$

where n is the number of bins used to calculate the PDF, Z_m is the frequency of values obtained for every bin by using the model data, and Z_0 is the frequency from the observed ones. Thereby, a Perkins SS of 1 means a perfect fit between modeled and observed data, and a value of 0 indicates that the modeled data are totally different to the observations. Because the shape of the PDF depends on the intervals selected, we used a bin of 1 for duration and magnitude and a bin of 0.5 for severity. Perkins SS was also computed by using the ERA

21698996, 2017, 3, Downloaded from https://agupubs.onlinelibrary.wiley.com/doi/10.1002/2016JD025683 by Readcube (Labtiva Inc.), Wiley Online Library on [27/01/2024]. See the Terms and Conditions (https://onlinelibrary.wiley.com/terms-and-conditions) on Wiley Online Library for rules of use; OA articles are governed by the applicable Creative Commons License

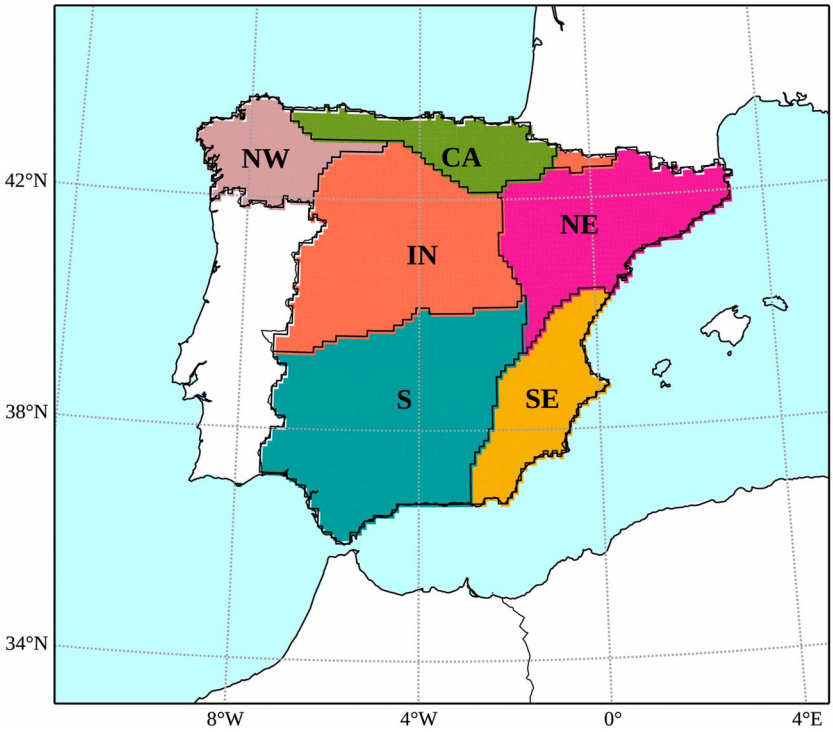

Figure 2. Homogeneous climate regions over Spain used for regional drought analysis: the northwestern (NW), Cantabrian (CA), northeastern (NE), interior (IN), southern (S), and southeastern (SE) regions.

data in order to use it to calculate the differences between both data as another measurement of added value of downscaled fields. The two-proportion z-test was applied to determinate those differences that were significant at the 95% confidence level.

2.4.2.3. Event Evaluations Based on the SPEI and SPI Indices

Finally, we also examined two different significant individual dry and wet episodes, analyzing the spatial behavior of the SPEI and SPI indices by using the WRF model and the driving data. The chosen events are a severe drought episode over the Iberian Peninsula during the year 2005, and a highly wet period occurred in 2009/2010. The results from this comparison could also show the benefit of using the dynamical downscaling method for detecting individual extreme events in dry and wet periods.

3. Results

3.1. Regionalization in Terms of Drought Indices

Three principal components were retained in accordance with the aforementioned criteria of selection when we used the regionalization method for 3 month SPEI that explained the 81.06% of the total variance of the data. Then, the factor loadings associated with the significant components were rotated and used to feed the hierarchical algorithm. The pseudo *F* test showed a local maximum for a six-cluster configuration, in accordance with the results reported in the work of *Vicente-Serrano* [2006], where a regionalization technique was performed over the Iberian Peninsula for the SPEI at 3 month time scale. Therefore, a six-cluster organization was chosen to apply the successive cluster analysis, and then a final configuration of six regions over Spain resulted in the following: the northwestern (NW) region, the Cantabrian (CA) region, the northeastern (NE) region, the interior (IN) region, the southern (S) region, and the southeastern (SE) region, as is shown in Figure 2.

The same regionalization procedure was used for the 12 month SPEI, and the results (not shown) for this time scale were very similar, and then, for simplicity, they were discarded. We also used the same regions to evaluate the SPI since both indices are very similar and our main goal is to have comparable regions in order to quantify the difference between the two indices from the downscaled fields and driving data, in terms of

21698996, 2017, 3, Downloaded from https://agupubs.onlinelibrary.wiley.com/doi/10.1002/2016JD025683 by Readcube (Labtiva Inc.), Wiley Online Library on [27/01/2024]. See the Terms and Conditions (https://onlinelibrary.wiley.com/terms-and-conditions) on Wiley Online Library for rules of use; OA articles are governed by the applicable Creative Commons License

drought indices. Therefore, in this study, the six main regions over Spain taken from the regionalization procedure applied to 3 month SPEI computed from mprmt data set were used to analyze both drought indices at the different time scales and for each data source.

3.2. Regional Drought Evaluation

Figure 3 illustrates the temporal evolution of the SPEI computed from mprmt, ERA, and WRFERA at 3 month time scale for the six main regions. The correlation coefficients (r) and RMSE between WRFERA (or ERA) and mprmt are shown in brackets. In general, although there is a substantial agreement between the observational SPEI and the ones computed with ERA and WRFERA, the fits to mprmt are slightly better for the downscaled SPEIs. This fact is corroborated in all regions by the higher correlation coefficients and lower RMSE values for WRFERA (r between 0.91–0.97 and 0.81–0.93 and RMSE between 0.21–0.36 and 0.34–0.53 for WRFERA and ERA, respectively). The south, interior, and northwestern regions appear to have the best fit, and the northeastern, southeastern, and Cantabrian regions the worst. Similar results are shown in Figure 4, which represents the temporal evolution of the 12 month SPEI from the different data sources. In this case, the best fit to the observational data provided by WRFERA is evident (r between 0.83 in the northeastern region and 0.98 in the south region and RMSE between 0.48 and 0.19 for the same regions). Particularly, this improvement is very remarkable for the northeastern region in the 2002–2005 period, for the interior region in the 2003–2005 period, and for the Cantabrian region in the 1989–1996 period. Conversely, the northeastern region shows a worse fit for WRFERA in the period of 1999–2001. Similar results (not shown) were found when we represented the regional SPI index at the time scales of 3 and 12 months.

A detailed analysis of the temporal correlation between both drought indices that resulted using simulated (ERA and WRFERA) data and the ones calculated from observed (mprmt) data is obtained from Figure 5. The SPEI and SPI calculated by using WRF outputs present higher correlation coefficients than the indices from the ERA data, with values above 0.83 in all regions. At 3 month time scale, the weakest correlation corresponds to the northeastern region for both indices and data sources, while the southern, northwestern, and interior regions registered the highest correlation coefficients. At 12 month time scale, these results are repeated, with a greater difference between the correlation coefficients of the downscaled drought indices and those found by using the driving. The results also showed that the SPEI presents a higher correlation than the SPI for both time scales and for both ERA and WRFERA in all regions (except for the southern region). Correlation coefficient differences between WRFERA and ERA (second columns in Figures 5a and 5b) display that WRF adds value with respect to the driving data. This improvement was higher for SPI and for 12 month time scale, being specially marked in the northeastern and Cantabrian regions. Regarding the comparison between indices, the results indicated that the highest relative improvement of SPI versus SPEI appeared in the northeastern region, which is 7.28% and 17.02% higher for SPI at 3 and 12 months, respectively. At 3 months, the improvement is 19.73% for SPI using WRFERA versus ERA and 12.45% for SPEI, while at 12 months, these improvements reach 57.16% and 40.14% for SPI and SPEI, respectively. In the Cantabrian region the relative improvement of SPI versus SPEI was also noticeable, being 3.56% and 8.40% higher at 3 and 12 month time scales (16.02% and 12.46% for SPI and SPEI, using WRFERA versus ERA, respectively, at 3 months, and 36.31% and 27.91% for SPI and SPEI, respectively, at 12 months). On the other hand, this improvement was not so obvious in the southeastern region, where the SPI improvement outperforms that obtained with SPEI in 1.67% and 0.74% at 3 and 12 months, respectively. Finally, the northwestern and interior regions showed intermediate values of improvements of SPI versus SPEI, about 2% for both time scales.

3.3. Local Drought Evaluation

In this section, we assess the added value of using WRF outputs for computing drought indices with respect to the driving data, directly comparing grid points in order to ensure that the results using the regionalization technique agree with the benefit of using downscaled field in further drought-projection studies.

3.3.1. Evaluation of Dry and Wet Episodes Using Drought Indices

The RMSEs between the simulated drought indices and the observed ones for every grid point are shown in Figure 6. Overall, the ERA RMSEs were higher than WRFERA RMSEs. The improvement provided by WRF is clearly shown in areas such as the Ebro Valley, which is located in the northeastern region. The added value of downscaled fields in this region is displayed for both time scales and for each index. The RMSE values for drought indices calculated on the 3 month time scale were between 0.3 and 0.9, approximately. Although the

21698996, 2017, 3, Downloaded from https://agupubs.onlinelibrary.wiley.com/doi/10.1002/2016JD025683 by Readcube (Labtiva Inc.), Wiley Online Library on [27/01/2024]. See the Terms and Conditions (https://onlinelibrary.wiley.com/terms-and-conditions) on Wiley Online Library for rules of use; OA articles are governed by the applicable Creative Commons License

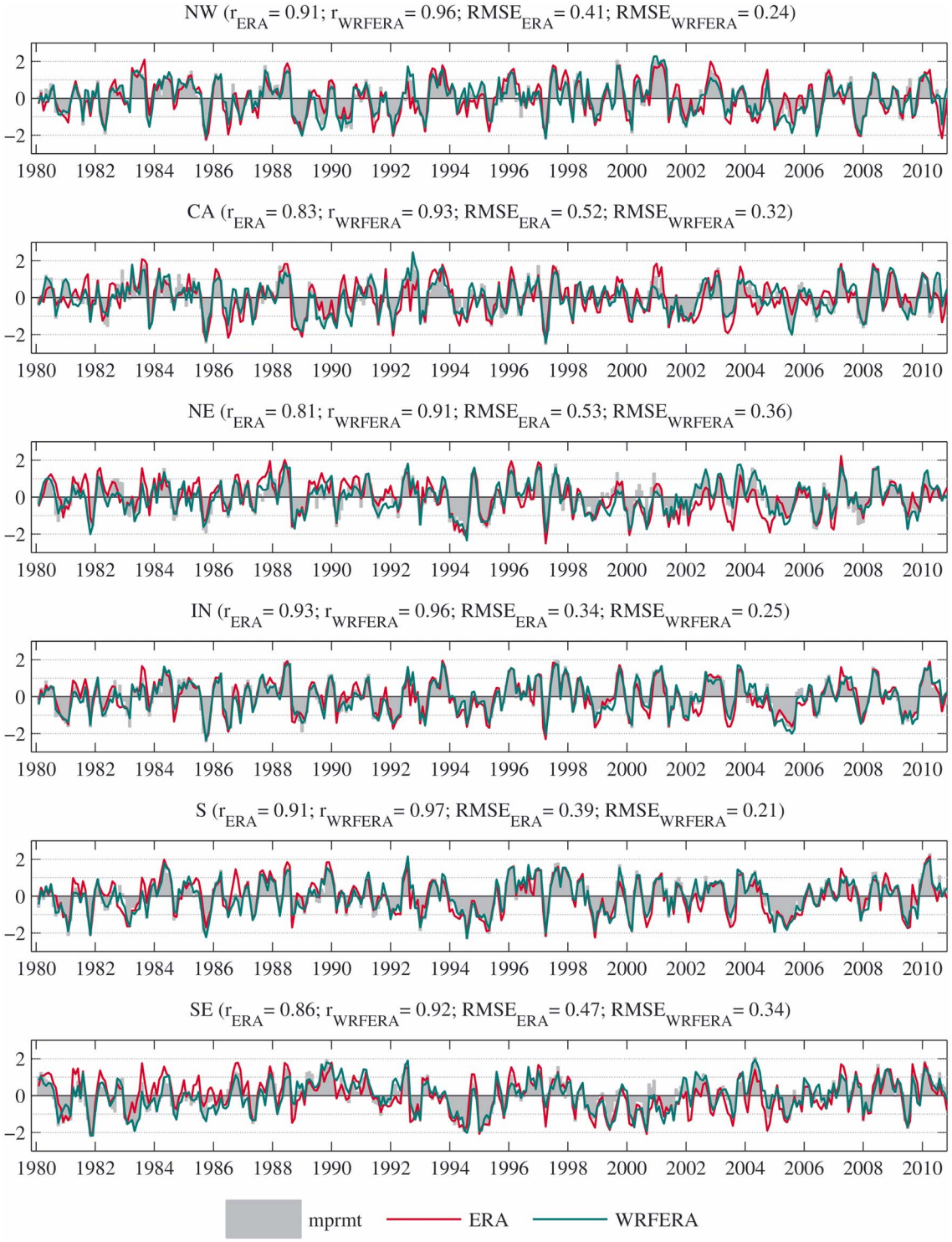

Figure 3. Temporal evolution of the 3 month SPEI from mprmt (grey columns), ERA (red lines), and WRFERA (green lines) data sets for the different regions. The spatial correlations (*r*) and the RMSE for ERA and WRFERA with respect to mprmt (in brackets).

spatial patterns for both indices were broadly very similar, the simulated SPEI shows better agreement than the simulated SPI with respect to the mprmt in terms of RMSEs. For instance, the Ebro Valley presents RMSE values about 0.7 and 0.85 for SPEI and SPI, respectively, when ERA drought indices were analyzed. The highest RMSE values, corresponding to the Cantabrian and the northeastern regions, were corrected, in general,

21698996, 2017, 3, Downloaded from https://agupubs.onlinelibrary.wiley.com/doi/10.1002/2016JD025683 by Readcube (Labtiva Inc.), Wiley Online Library on [27/01/2024]. See the Terms and Conditions (https://onlinelibrary.wiley.com/terms-and-conditions) on Wiley Online Library for rules of use; OA articles are governed by the applicable Creative Commons License

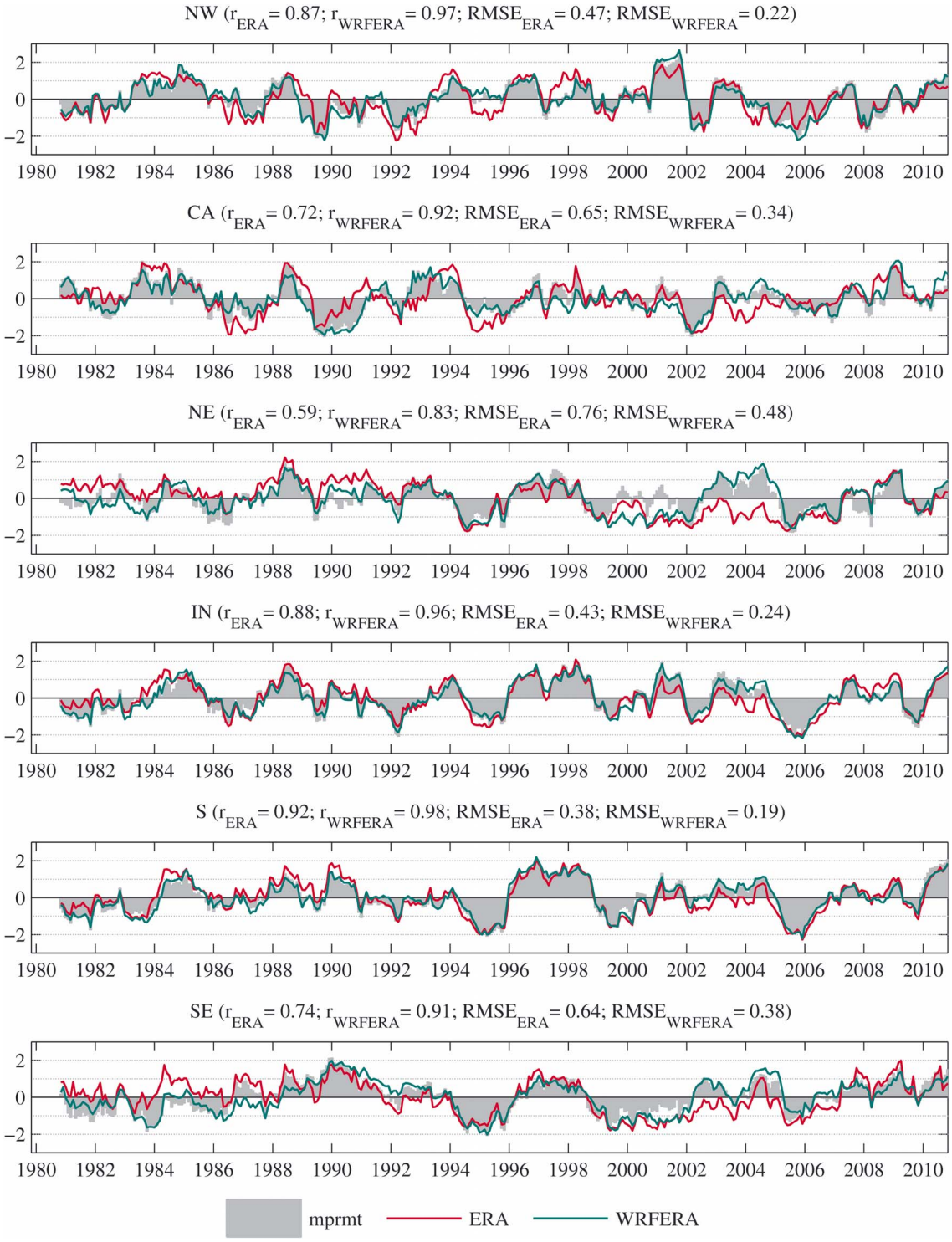

Figure 4. As in Figure 3 but for 12 month SPEI.

using the downscaled fields. On the other hand, the lowest RMSE values corresponded to the northwestern, south, and interior regions of Spain, as can be seen in Figure 6. At a time scale of 12 months, the RMSE presented a larger range of values (between 0.2 and 1.2). For this time scale, the improvement for SPEI with respect to the SPI was not evident as that occurred at 3 months since the two indices show a similar RMSE in most areas of Spain. For both indices, WRFERA presented the largest RMSEs (>1) in areas located in the

21698996, 2017, 3, Downloaded from https://agupubs.onlinelibrary.wiley.com/doi/10.1002/2016JD025683 by Readcube (Labtiva Inc.), Wiley Online Library on [27/01/2024]. See the Terms and Conditions (https://onlinelibrary.wiley.com/terms-and-conditions) on Wiley Online Library for rules of use; OA articles are governed by the applicable Creative Commons License

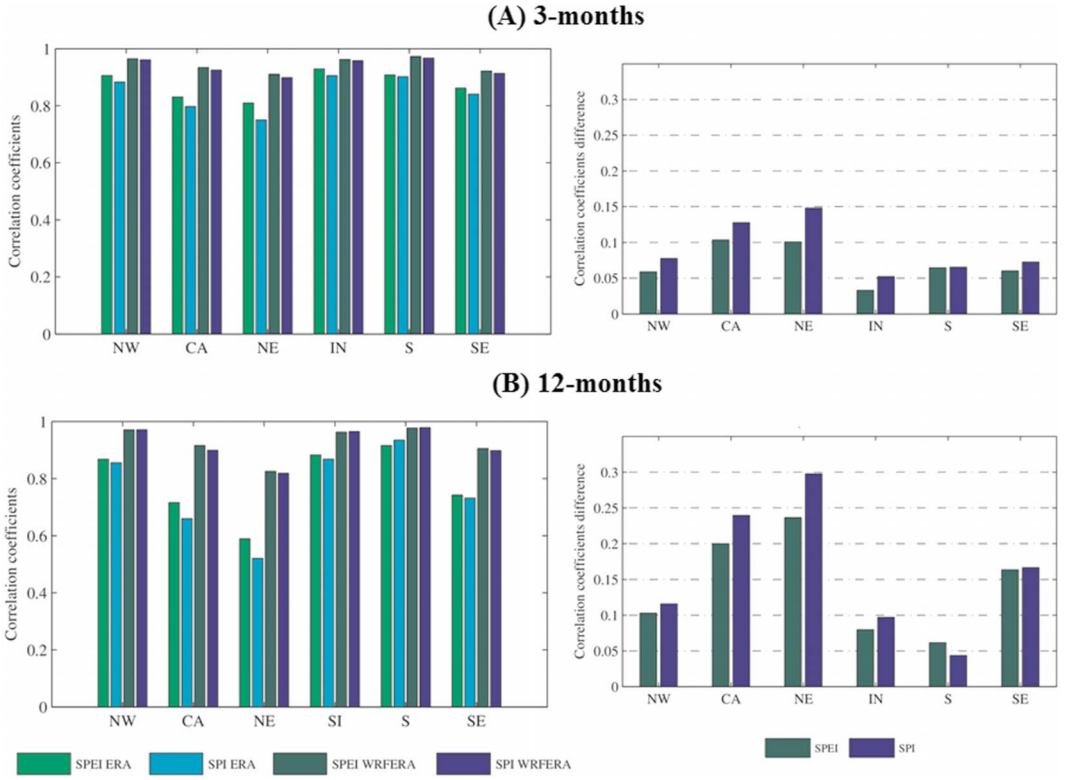

Figure 5. Correlation coefficients between regionalized drought indices computed by using ERA and WRFERA and the indices computed from mprmt and correlation coefficient differences (WRFERA minus ERA) at (a) 3 month and (b) 12 month time scales.

Cantabrian and the northeastern regions such as the Ebro Valley, the Pyrenees, and the Cantabrian range (Figure 1b). However, the WRFERA simulations were broadly better than the ERA ones. The RMSE values also improved by using WRF in most of the rest of Spain, as is shown in Figure 6. These results suggest that the simulated drought indices using WRF outputs are able to reproduce the observed indices, showing remarkable improvements with respect to the simulations only with ERA, presenting an added value that depends on the time scale used. For both time scales, the RMSE values for SPEI and SPI indices obtained with WRFERA were very similar, while the errors are greater for SPI than for SPEI when ERA data were used. Thus, the improvement provided by using WRF for SPI was higher than that for SPEI. The results of the analysis are in accordance with those obtained for the temporal correlation coefficients for each region shown in Figure 5.

The spatial correlation coefficients between one grid and another one along the south-to-north (Figure 7 a) and west-to-east (Figure 7b) directions, with a lag of 0.4°, using the drought indices from mprmt, ERA, and WRFERA, were calculated. Figure 7 displays the spatial correlation from mprmt (first row) and the differences from ERA (second row) and WRFERA (third row) with respect to mprmt. A positive difference means that two points from the simulated drought indices are more similar between them than the same points from the observational data. So for topographically complex areas, this implies that the simulated drought indices are not able to capture the spatial variability. Conversely, a negative difference means that the simulated drought indices are more sensitive to spatial variability. For mprmt, the spatial correlations showed a noticeable decrease over the Cantabrian range, oriented in the west-to-east direction, for the latitudinal lag. For the longitudinal lag, the main mountain ranges (Figure 1b), oriented in the south-to-north direction, were adequately displayed. Additionally, high spatial correlations (above 0.9) were found over the Central Plateaus and the Guadalquivir Valley. In general, the differences of the spatial correlations between ERA and mprmt are positive, showing that ERA is not able to capture the spatial variations and local characteristics in terms of drought indices in the main mountain ranges of Spain. However, WRFERA

21698996, 2017, 3, Downloaded from https://agupubs.onlinelibrary.wiley.com/doi/10.1002/2016JD025683 by Readcube (Labtiva Inc.), Wiley Online Library on [27/01/2024]. See the Terms and Conditions (https://onlinelibrary.wiley.com/terms-and-conditions) on Wiley Online Library for rules of use; OA articles are governed by the applicable Creative Commons License

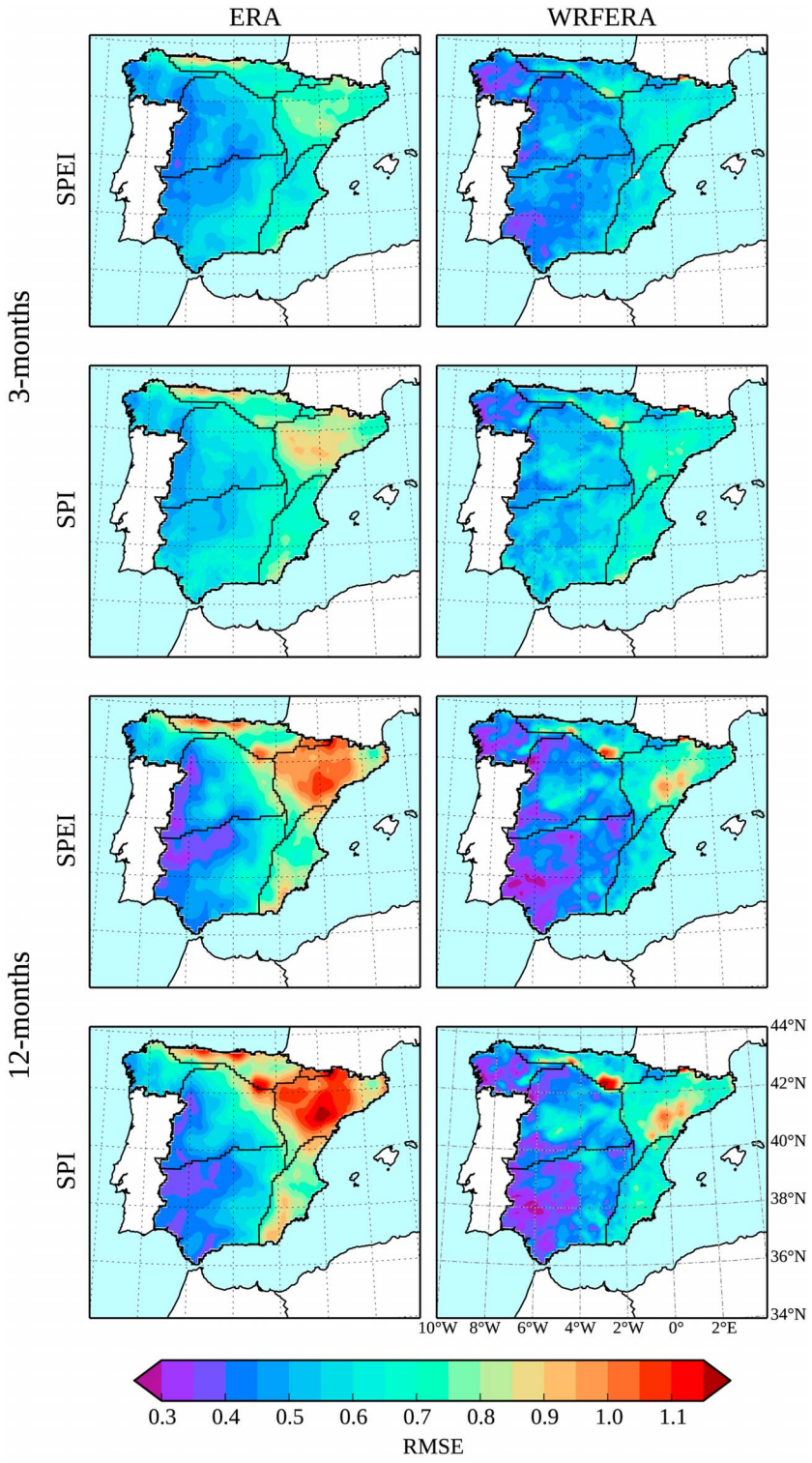

Figure 6. Root-mean-square errors (RMSEs) between the drought indices computed from ERA and WRFERA data sets with respect to those from mprmt, for the SPEI and the SPI at 3 and 12 month time scales.

adequately reproduces this spatial variability, even more than the observational data (the differences are negative in general). For instance, it was able to capture the main spatial patterns of drought in a region as the Central Massif. These results are similar for both SPI and SPEI indices and more evident at 12 month time scale.

21698996, 2017, 3, Downloaded from https://agupubs.onlinelibrary.wiley.com/doi/10.1002/2016JD025683 by Readcube (Labtiva Inc.), Wiley Online Library on [27/01/2024]. See the Terms and Conditions (https://onlinelibrary.wiley.com/terms-and-conditions) on Wiley Online Library for rules of use; OA articles are governed by the applicable Creative Commons License

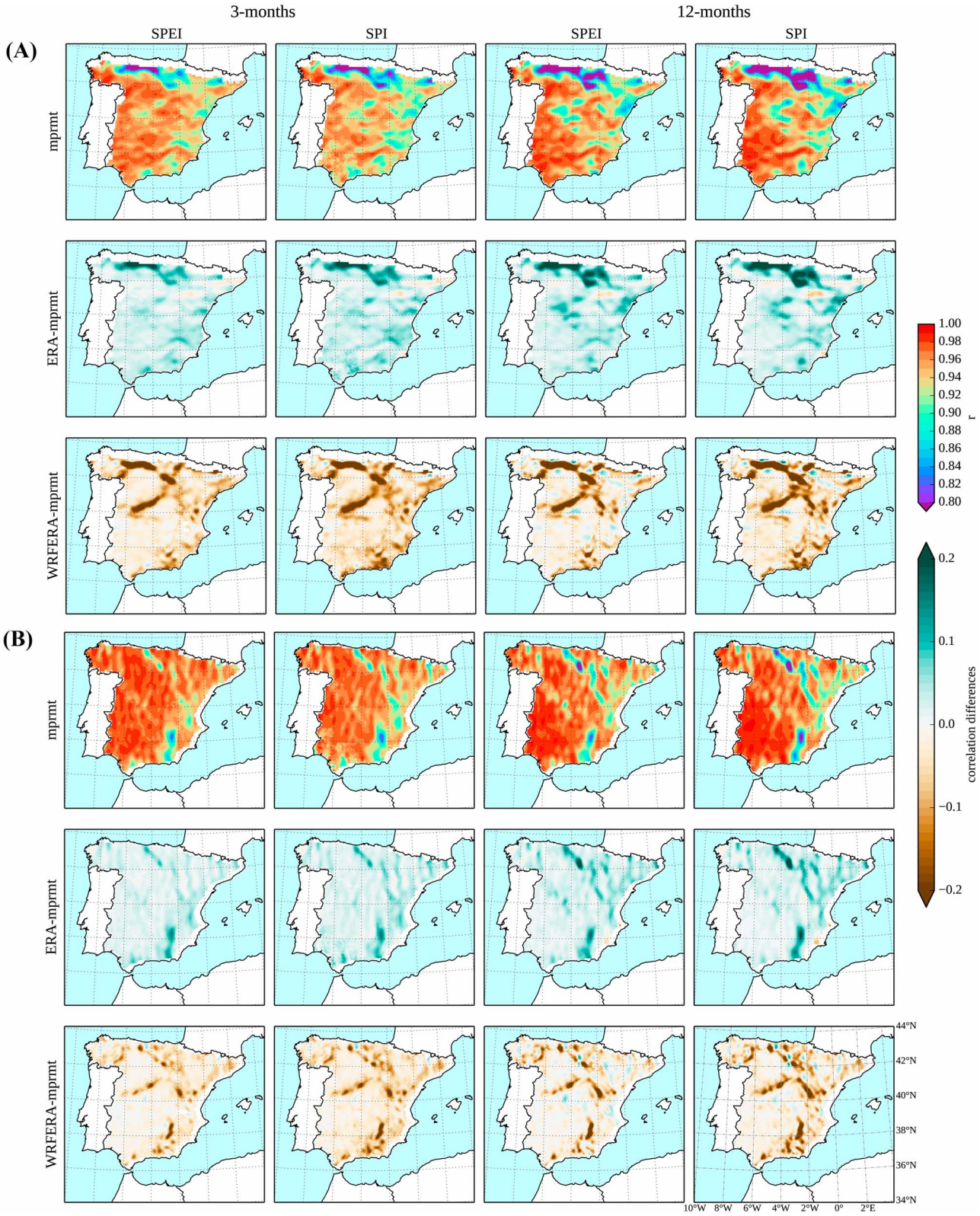

Figure 7. Spatial correlation coefficients from mprmt and the differences between ERA and WRFERA with respect to mprmt, for a lag of 0.4° along the (a) south-to-north and (b) west-to-east directions.

21698996, 2017, 3, Downloaded from https://agupubs.onlinelibrary.wiley.com/doi/10.1002/2016JD025683 by Readcube (Labtiva Inc.), Wiley Online Library on [27/01/2024]. See the Terms and Conditions (https://onlinelibrary.wiley.com/terms-and-conditions) on Wiley Online Library for rules of use; OA articles are governed by the applicable Creative Commons License

21698996, 2017, 3, Downloaded from https://agupubs.onlinelibrary.wiley.com/doi/10.1002/2016JD025683 by Readcube (Labtiva Inc.), Wiley Online Library on [27/01/2024]. See the Terms and Conditions (https://onlinelibrary.wiley.com/terms-and-conditions) on Wiley Online Library for rules of use; OA articles are governed by the applicable Creative Commons License

Figure 8 depicts the CSI for events with SPI or SPEI above 1 and below −1 from WRFERA and ERA with respect to the mprmt. The significant relative differences (WRFERA *minus* ERA) between them regarding ERA at the 95% confidence level are also shown (third column). Using these differences, we can compare and quantify the WRF ability to characterize moderate and extreme wet and dry periods. At a 3 month time scale, the two indices present CSI values of between 20% and 80%, with the largest CSI values in the northwestern, interior, and south of Spain. Conversely, the lowest values correspond to the eastern region. With respect to the comparison between both indices, the results suggest that the SPI slightly outperformed the SPEI. The comparison between WRFERA and ERA using the CSI relative differences showed that downscaled fields outperformed the driving data in terms of drought indices in areas located in the northwestern, Cantabrian, and northeastern regions, with improvements about 60% at 3 month time scale, these improvements being more noticeable for SPI. At 12 month time scale, the two indices, which presented very similar results, showed more regions with higher CSI values, especially in the southwestern region, with CSIs of about 80%. By contrast, the worst values of CSI were in eastern Spain, as occurred at 3 month time scale. For the relative differences between WRFERA and ERA, WRF provides a higher added value, with improvements above 100% in regions located in the north of Spain (e.g., the Cantabrian coast, Pyrenees, Galician Massif, northern central plateau, and Ebro Valley). When comparing CSIs based on SPEI with those obtained by using SPI, the results suggest that the greatest added value corresponds to the SPI, as it is shown in Figure 8. Therefore, the CSI analysis suggests that the ability of the WRF model to simulate drought indices depends on the time scale (higher at 12 months), and in general, the SPI performs better than the SPEI, in agreement with the RMSE results. Furthermore, for both indices and time scales, the RMSE and the CSI showed similar spatial patterns throughout Spain.

3.3.2. Assessing the Characteristics of Drought Events

Magnitude, duration, and severity parameters of droughts from SPEI and SPI values below 0 were also computed. Figure 9 illustrates the magnitude averaged for the entire study period for simulated and observed drought events. The spatial RMSE in reference to the mprmt was also calculated (shown in brackets) in order to quantify its spatial similarity with observations. The average drought magnitude presents values between 2.5 and 4 at 3 month time scale and between 6 and 16 at 12 month time scale. In general, at a 3 month time scale, WRF does not seem to provide any clear improvement with respect to the driving data. This unclear result can be also observed in the spatial RMSE, which is even slightly worse for SPEI WRFERA. However, the improvement provided by downscaled fields seems greater when we used longer time scales, showing spatial patterns from WRFERA at 12 months more similar to those from the mprmt, as can be seen for southeastern Spain. This finding is also shown for the spatial RMSE, with lower values for WRFERA simulations. We drew similar conclusions when we compared the average duration of drought events (not shown), which presented values between 3 and 5 months and between 7 and 17 months at 3 and 12 month time scales, respectively. As occurred with the magnitude, the average duration showed a higher RMSE at 3 month SPEI from WRFERA, so in general, it seems that WRF does not provide clear improvements in terms of drought duration and magnitude on average, using a time scale of 3 months. The average drought severity (Figure 10), with values between 0.9 and 1.35 and between 0.5 and 1.5 at 3 and 12 month time scales, respectively, is overestimated for ERA simulations in most of Galicia for both indices and time scales. Nevertheless, WRF seems to correct this inaccuracy, so that the average severity in this area from WRFERA is more similar to that found with mprmt. In general, the results show that WRFERA provides better results for the average drought severity, in agreement with spatial RMSE values.

According to the Perkins SS for duration distribution, Figure 11 compares the Perkins SS for SPEI and SPI by using ERA and WRFERA with respect to mprmt, and the significant relative differences between them (relative to ERA) expressed in percentage, at 95% confidence level (third column). These differences also provide a measurement of added value for WRF outputs. Positive differences mean that WRF outputs add value in terms of drought characteristics. Conversely, a negative difference means that the driving data outperform downscaled fields. While the Perkins SS was between 60% and 100% at a 3 month time scale in most of Spain, the Perkins SS at 12 months was below 70%. Looking at the relative differences between WRFERA and ERA, we conclude that the benefit of using downscaled fields depends on the index, the time scale, and the region considered. The number of grid points with significant positive differences (red dots) and the number of those grid points with significant negative differences (blue dots) as well as the average of these relative differences are shown in Table 1. At 3 month time scale, the number of points with positive

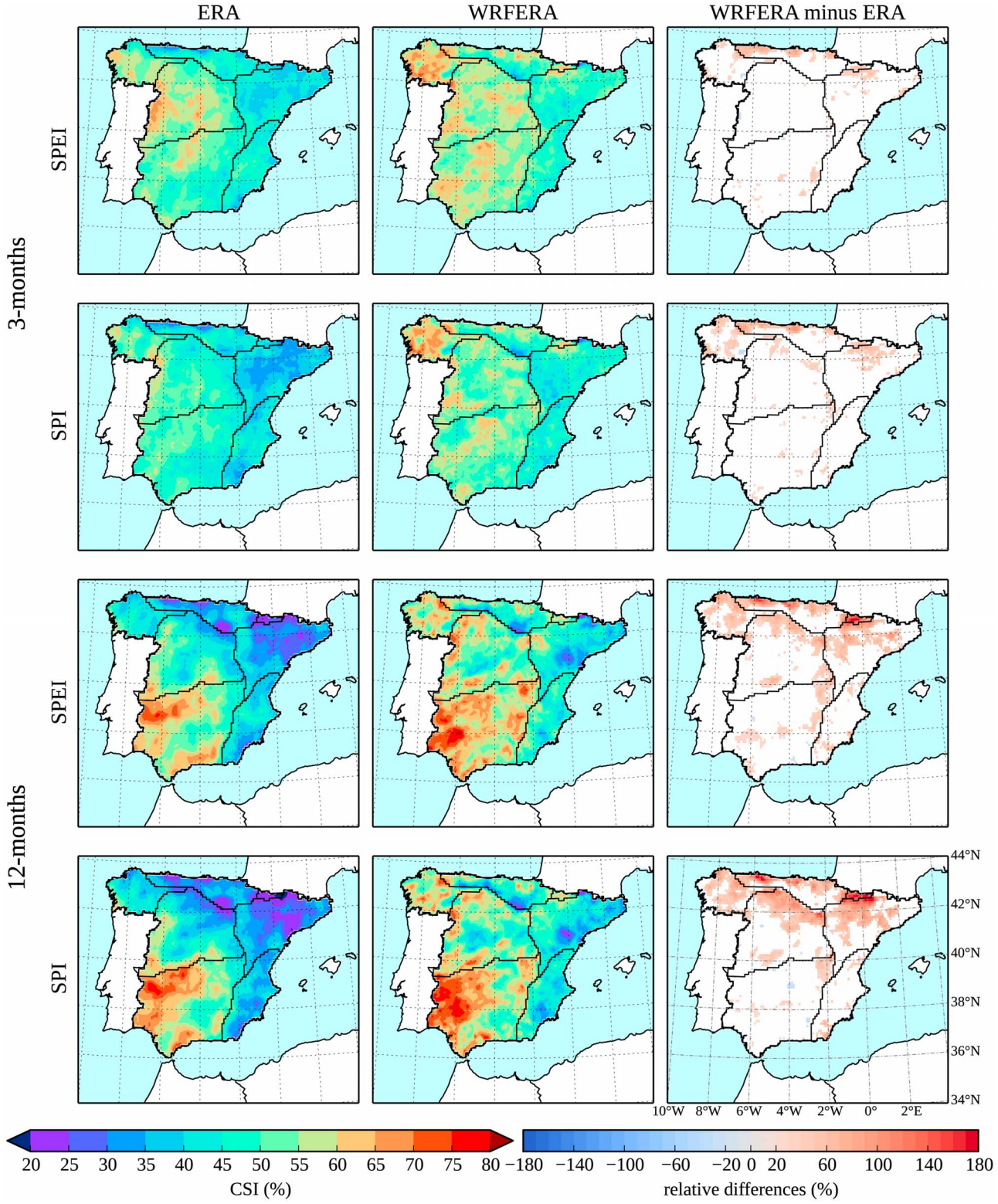

Figure 8. Critical Success Index (CSI) between simulated (ERA and WRFERA) and observed (mprmt) SPEI and SPI at 3 and 12 month time scales. The significant relative CSI differences (WRFERA minus ERA) at the 95% confidence level (third column).

21698996, 2017, 3, Downloaded from https://agupubs.onlinelibrary.wiley.com/doi/10.1002/2016JD025683 by Readcube (Labtiva Inc.), Wiley Online Library on [27/01/2024]. See the Terms and Conditions (https://onlinelibrary.wiley.com/terms-and-conditions) on Wiley Online Library for rules of use; OA articles are governed by the applicable Creative Commons License

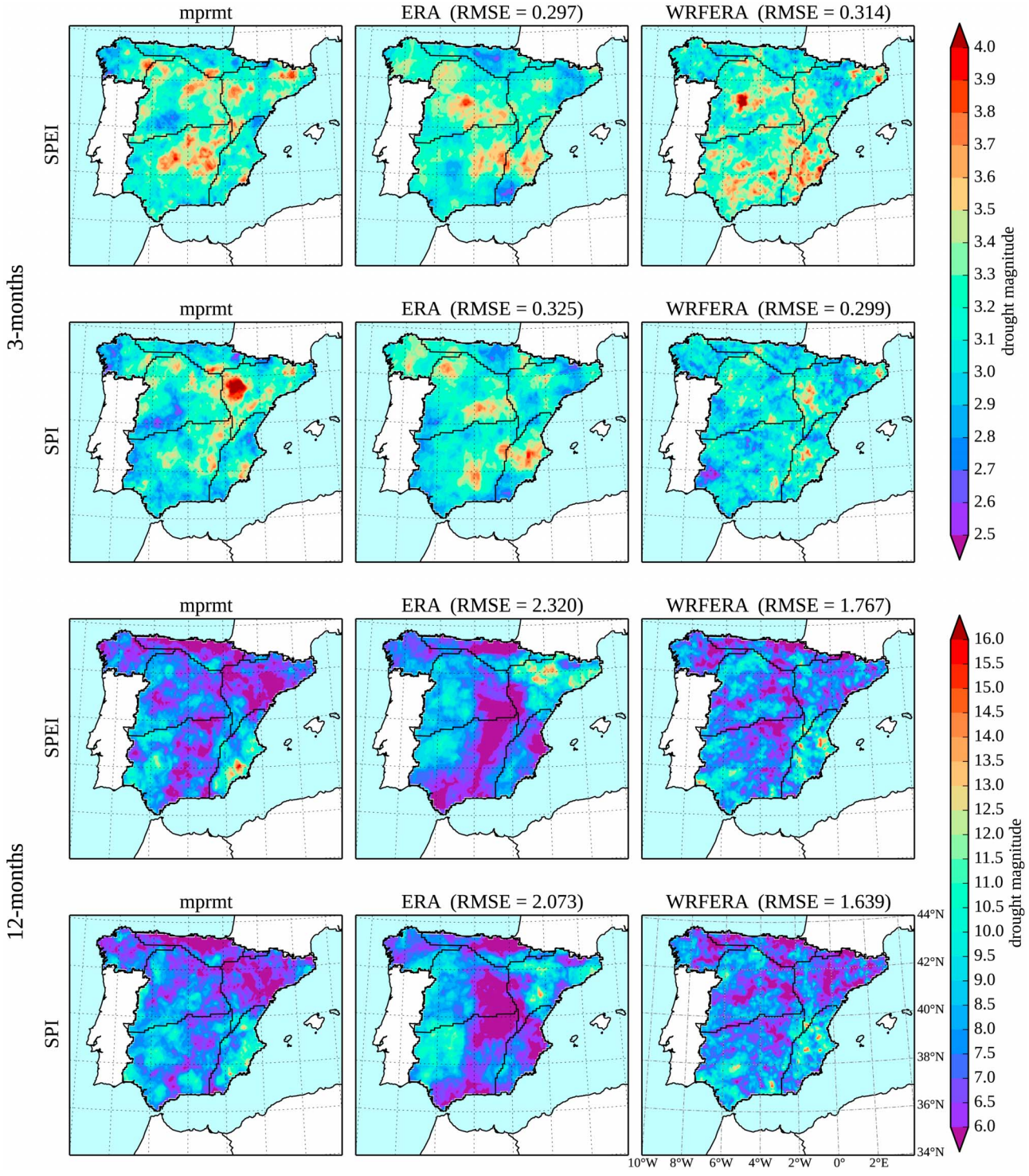

Figure 9. Average drought magnitude from mprmt, ERA, and WRFERA, calculated by using SPEI and SPI indices at 3 and 12 month time scales. The spatial RMSE with respect to mprmt (in brackets).

values was larger than that with negative values for SPI Perkins SS differences. Nonetheless, the SPEI Perkins SS shows a number of points in which ERA performs better than WRFERA. In this regard, the results suggested that the SPEI based on ERA data captures better the behavior of the individual drought events in terms of duration. However, comparing the average of the relative differences results in evidence that the

21698996, 2017, 3, Downloaded from https://agupubs.onlinelibrary.wiley.com/doi/10.1002/2016JD025683 by Readcube (Labtiva Inc.), Wiley Online Library on [27/01/2024]. See the Terms and Conditions (https://onlinelibrary.wiley.com/terms-and-conditions) on Wiley Online Library for rules of use; OA articles are governed by the applicable Creative Commons License

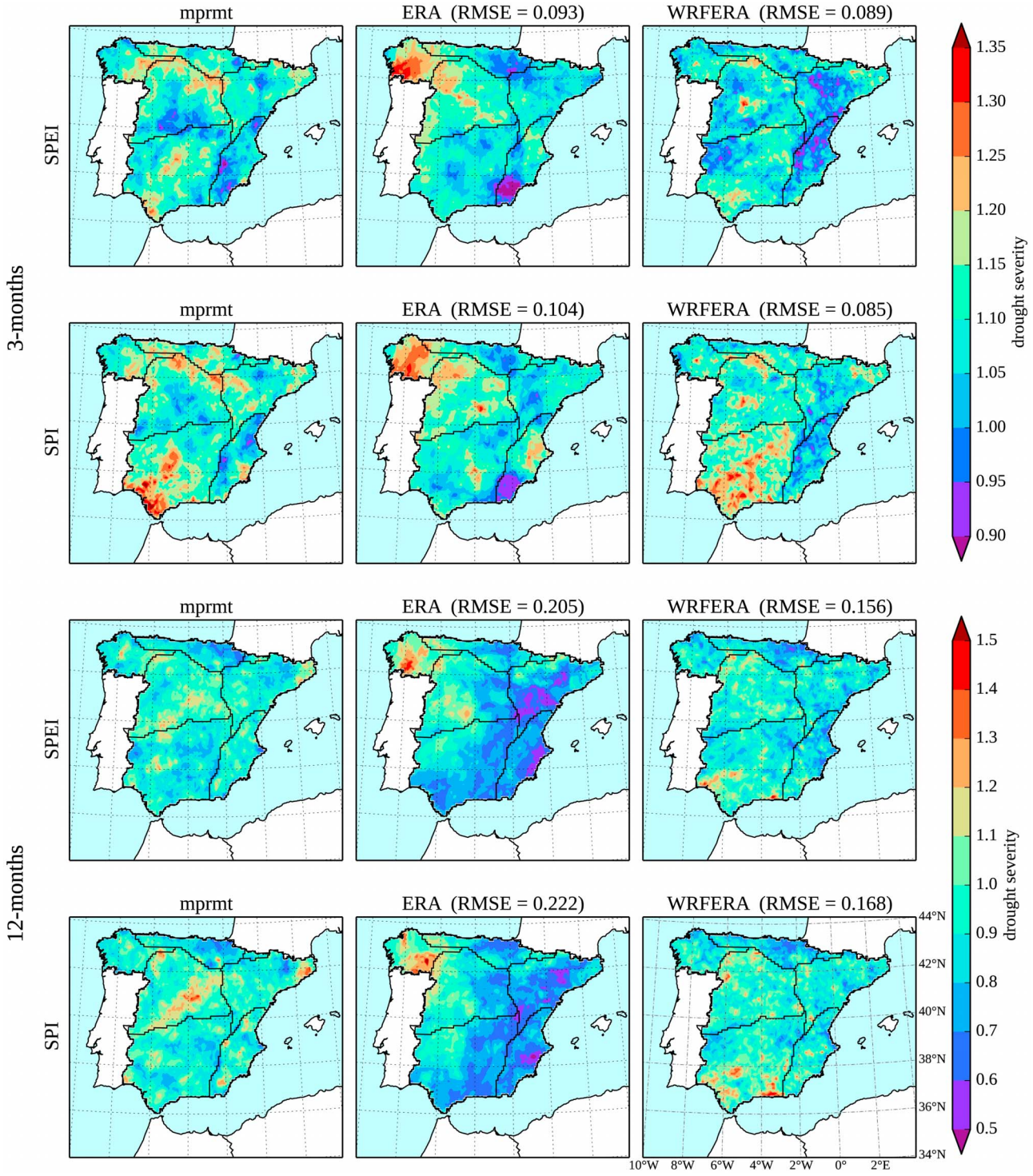

Figure 10. As in Figure 8 but for the average drought severity.

improvement provided by WRF is always higher. The improvement provided by high-resolution data is more noticeable at 12 months than at 3 months, since the number of points with significant positive differences is higher, the average differences also being greater for both indices at 12 month time scale (see Table 1). Therefore, these results suggest that the benefit of using downscaled fields to detect drought duration distribution is higher at longer time scales and for the SPI index.

21698996, 2017, 3, Downloaded from https://agupubs.onlinelibrary.wiley.com/doi/10.1002/2016JD025683 by Readcube (Labtiva Inc.), Wiley Online Library on [27/01/2024]. See the Terms and Conditions (https://onlinelibrary.wiley.com/terms-and-conditions) on Wiley Online Library for rules of use; OA articles are governed by the applicable Creative Commons License

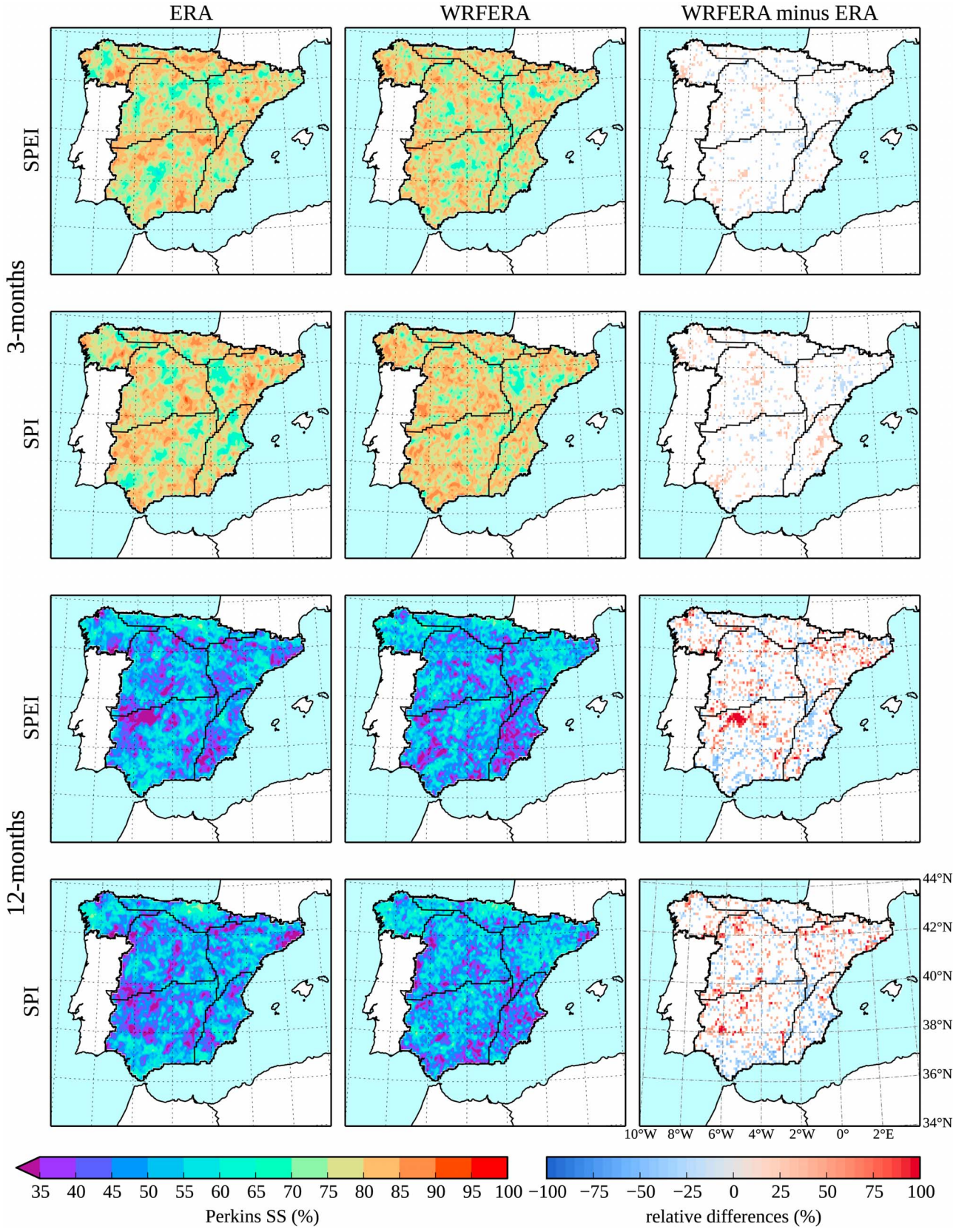

Figure 11. Perkins Skill Score (SS) for probability distribution functions of drought duration for the SPEI and SPI at 3 and 12 month time scales from ERA and WRFERA with respect to those computed from mprmt and significant relative differences (WRFERA minus ERA) between them at the 95% confidence level.

21698996, 2017, 3, Downloaded from https://agupubs.onlinelibrary.wiley.com/doi/10.1002/2016JD025683 by Readcube (Labtiva Inc.), Wiley Online Library on [27/01/2024]. See the Terms and Conditions (https://onlinelibrary.wiley.com/terms-and-conditions) on Wiley Online Library for rules of use; OA articles are governed by the applicable Creative Commons License

Table 1. Number of Grid Points With Significant Relative Differences for Duration, Magnitude, and Severity of Droughts and the Average of These Relative Differences

	WRFERA Minus ERA > 0		WRFERA Minus ERA < 0	
	No. of Grid Points	Average (%)	No. of Grid Points	Average (%)
		Duration		
SPEI_03	229	20.54	281	17.06
SPI_03	373	21.73	236	17.25
SPEI_12	766	59.48	618	34.94
SPI_12	780	55.22	566	34.78
		Magnitude		
SPEI_03	342	22.95	340	18.41
SPI_03	654	24.55	225	18.71
SPEI_12	897	60.76	803	36.85
SPI_12	842	57.13	858	36.80
		Severity		
SPEI_03	612	13.09	740	11.95
SPI_03	1088	13.49	468	11.54
SPEI_12	1569	26.06	918	20.75
SPI_12	1647	24.45	930	20.86

The Perkins SS magnitude (figure not shown) also displayed higher values at 3 month than at 12 month time scales (for 3 months, Perkins SS was between 60% and 100% and below 70% for 12 months). The added value of downscaled fields again depending on the index, time scale, and region was considered. Overall, the relative differences show that the added value is not obvious since the number of grid points with positive and negative values is similar, except for the SPI at 3 months, which shows a noticeable number of points with positive differences (Table 1). In terms of average differences, the improvements are high, especially for 12 month drought indices.

Regarding the severity of the drought events (Figure 12), the Perkins SS showed values of between 70% and 98% at 3 month time scale and between 55% and 100% at 12 month time scale. With respect to the relative differences, the SPEI index shows a lower number of significant positive differences at both time scales, while SPI again shows a higher number of positive values. These differences, in average, are higher for both indices as happens in the duration parameter (Table 1). Again, the results suggest that the benefit of using WRF outputs depending on the index, time scale, and region is considered. For instance, note the high added value presented in the northeastern region, especially for 12 month SPEI.

3.3.3. Event Evaluations Based on the SPEI and SPI Indices

Finally, the behavior of the drought indices during different extreme wet and dry episodes using downscaled fields was investigated. The interest of this study is because these events are associated with mechanisms in large-scale atmospheric circulation, which is already well simulated by the driving data. Thus, we are able to test the added value provided by WRF outputs to detect severe drought events.

First, we focused on a severe drought episode over the Iberian Peninsula during the year 2005. This drought event, which began in November 2004, was considered the driest event in the last 140 years [*García-Herrera et al.*, 2007], producing low historic records of accumulated precipitation. This intense dry event occurred by the combination of different mechanisms: a positive North Atlantic Oscillation (NAO) index between November 2004 and January 2005, followed by a negative phase of East Atlantic pattern in February and a negative NAO phase caused by an intense and anomalous blockage displaced from its usual location from March 2005 [*García-Herrera et al.*, 2007]. Figure 13 depicts the spatial distribution of drought indices from mprmt, ERA, and WRFERA corresponding to September 2005 at 3 and 12 month time scales. The correlation between patterns is displayed in brackets, showing the standard Pearson's correlation coefficients between the ERA and WRFERA drought indices with respect to those from mprmt. Although ERA reliably captured the broad pattern of the drought, showing correlation values of spatial patterns of 0.441 and 0.341 for SPEI and SPI, respectively, at a 3 month time scale (Figure 13a), WRF provided a substantial improvement, presenting higher correlations with values of 0.757 and 0.697 for the SPEI and SPI, respectively. On the northeastern region, moderate-to-severe drought, i.e., the SPEI and SPI below −1, resulted from ERA drought indices, while from mprmt data showed normal to wet episodes, i.e., SPEI and SPI above 1. However, WRF simulations

21698996, 2017, 3, Downloaded from https://agupubs.onlinelibrary.wiley.com/doi/10.1002/2016JD025683 by Readcube (Labtiva Inc.), Wiley Online Library on [27/01/2024]. See the Terms and Conditions (https://onlinelibrary.wiley.com/terms-and-conditions) on Wiley Online Library for rules of use; OA articles are governed by the applicable Creative Commons License

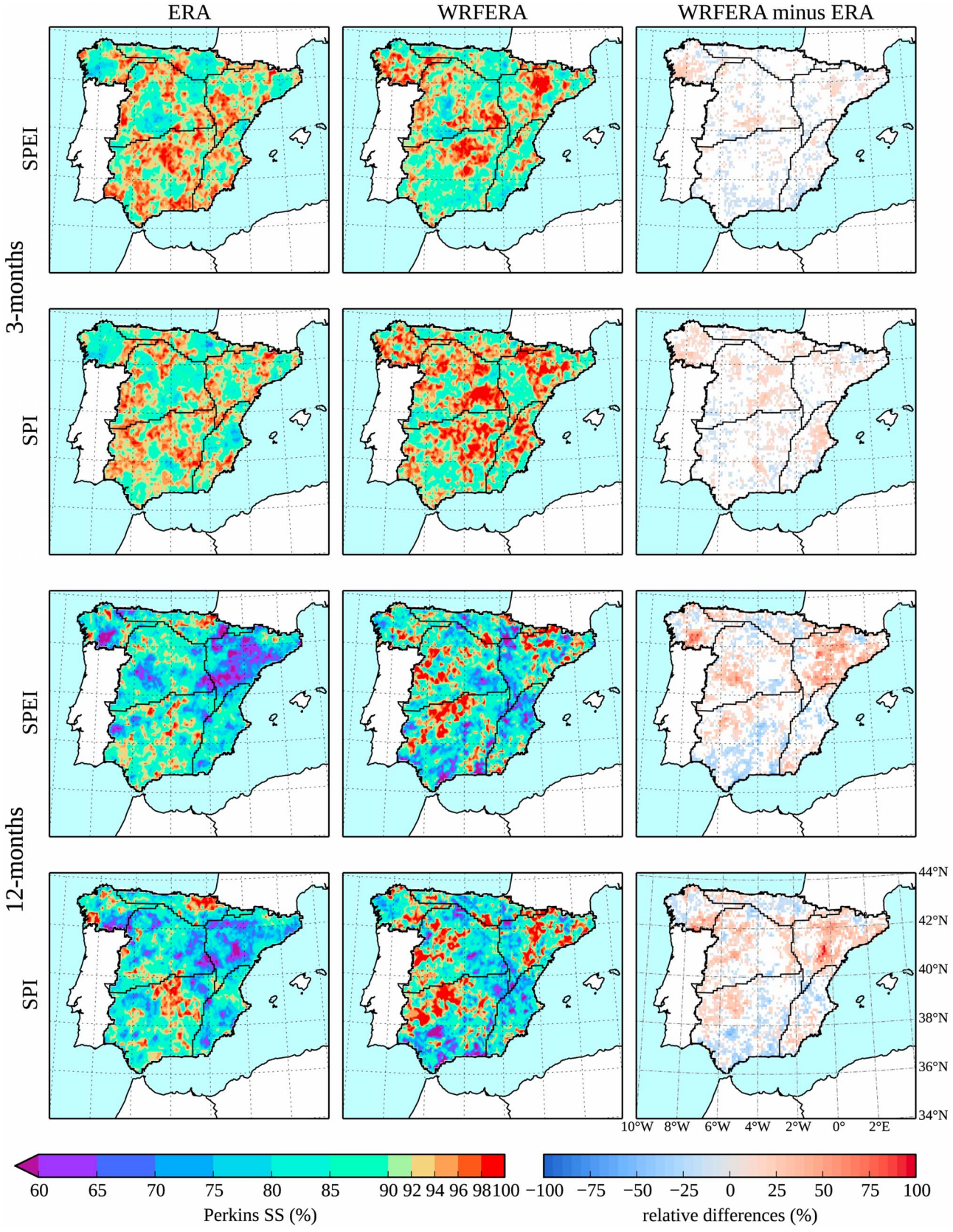

Figure 12. As in Figure 10 but for the probability distribution function of drought severity.

21698996, 2017, 3, Downloaded from https://agupubs.onlinelibrary.wiley.com/doi/10.1002/2016JD025683 by Readcube (Labtiva Inc.), Wiley Online Library on [27/01/2024]. See the Terms and Conditions (https://onlinelibrary.wiley.com/terms-and-conditions) on Wiley Online Library for rules of use; OA articles are governed by the applicable Creative Commons License

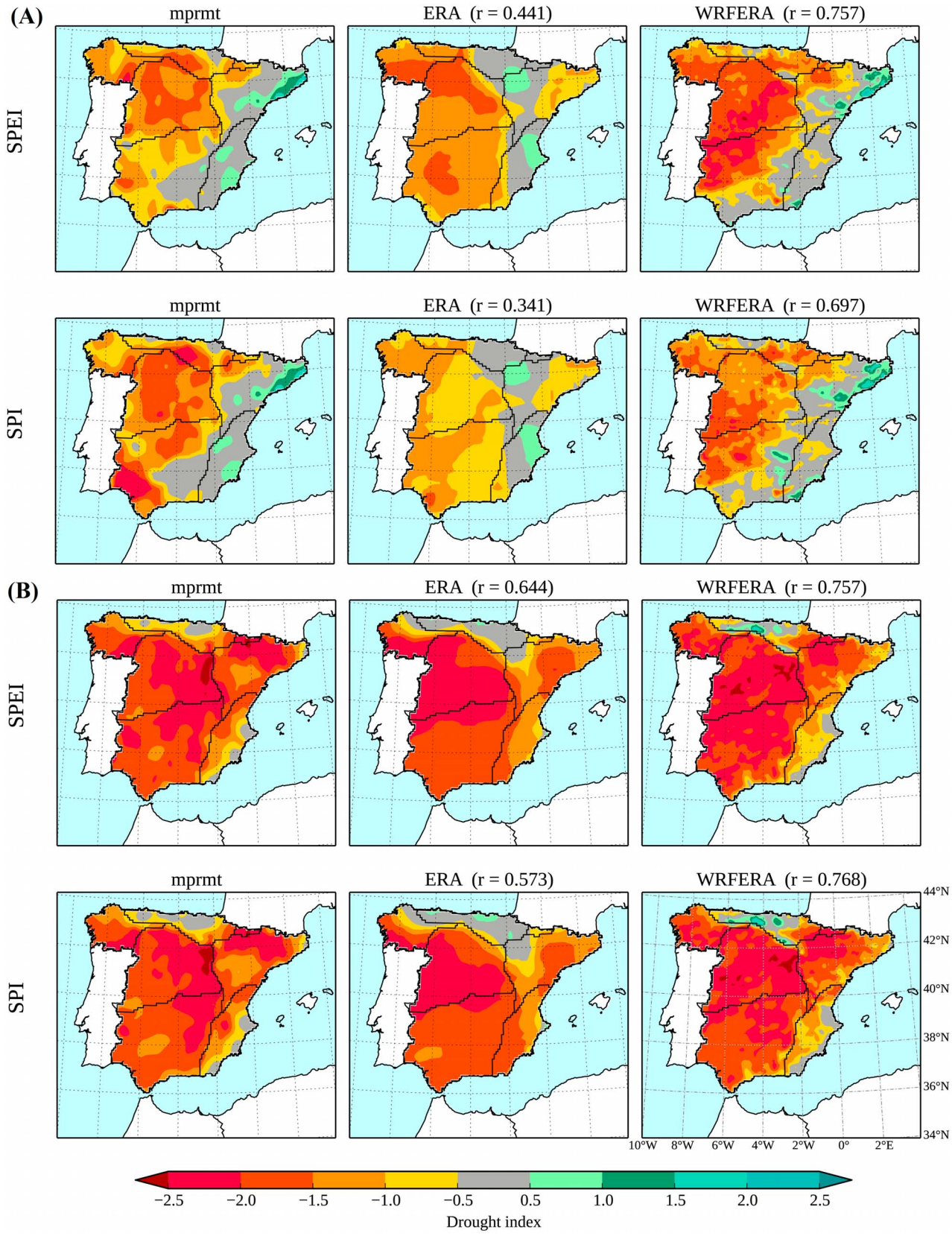

Figure 13. Drought indices ending in September 2005 calculated from mprmt, ERA, and WRFERA, at (a) 3 month and (b) 12 month time scales. The spatial correlation coefficients of the simulated indices with respect to mprmt (in brackets).

21698996, 2017, 3, Downloaded from https://agupubs.onlinelibrary.wiley.com/doi/10.1002/2016JD025683 by Readcube (Labtiva Inc.), Wiley Online Library on [27/01/2024]. See the Terms and Conditions (https://onlinelibrary.wiley.com/terms-and-conditions) on Wiley Online Library for rules of use; OA articles are governed by the applicable Creative Commons License

correctly represent the behavior of the mprmt drought indices, showing that, particularly for this region, WRF adds value relative to ERA. Furthermore, the results also show that WRF properly reproduced the transition drought pattern between the Mediterranean strip and the interior plateau, with significant improvements for the Ebro Valley. By contrast, in the southwestern region, an extreme drought is observed, which it is not captured by WRFERA at the 3 month time scale in part of the area affected. In the comparison between the drought indices, the SPEI and SPI showed similar drought spatial patterns, although the SPEI presented slightly higher correlation values with the observed drought events for most cases. At 12 month time scale, both indices presented very similar spatial patterns, as reflected by Figure 13b. As expected, ERA showed suitable results (with correlation coefficients between spatial patterns of 0.644 and 0.573 for the SPEI and SPI, respectively), but the drought indices simulated by using WRFERA improved locally with respect to the mprmt, presenting correlation values of 0.757 for SPEI and 0.768 for SPI. Conversely, on the Cantabrian region, WRF overestimates the wet conditions. Therefore, in general, these results suggest that WRF provides an improvement at the local scale for the 2005 extreme drought event.

Second, to evaluate the ability of the WRF to simulate extreme wet episodes, we have assessed the performance of the drought indices during a highly wet event. The winter of 2009/2010 was characterized by one of the most extreme negative NAO phases during the last 150 years, triggering the highest amounts of winter precipitation on most of the Iberian Peninsula [*Vicente-Serrano et al.*, 2011b]. To evaluate the ability of WRF to simulate this wet winter in Spain, we used the two drought indices computed ending in March 2010 (Figure 14a). In general, ERA and WRFERA agreed well with respect to the mprmt. Again, WRF captured this wet episode better than ERA alone, for both 3 and 12 month time scales, for most of Spain. Specifically, at 3 months, the added value of using WRF proved higher, resulting in spatial pattern correlation coefficients of 0.744 and 0.748 for WRFERA SPEI and WRFERA SPI, respectively, versus 0.584 and 0.586 for ERA SPEI and ERA SPI, respectively. Although some errors persist, such as the overestimations in the Ebro Valley and the underestimations in the south, the WRF model is nevertheless able to capture suitably the wet pattern along the northwestern region by using both indices. For this wet episode in particular, the SPI appeared to slightly outperform the SPEI. Figure 14b compares the drought indices that correspond to November 2010 at a 12 month time scale. Although ERA and WRFERA reliably captured the main wet pattern for the year 2010, WRFERA agreed better with respect to observations in general, except for some areas in the Cantabrian region. Differences between ERA and WRFERA are smaller at 3 month time scale, as is reflected by the spatial pattern correlation coefficients (0.597 for ERA SPEI versus 0.639 for WRFERA SPEI and 0.618 for ERA SPI versus 0.681 for WRFERA SPI).

4. Conclusions and Discussion

In this study, the WRF model has been used to assess the model's capability to simulate wet and dry periods for two different drought indices, SPEI and SPI, over Spain. The goal is to assess the improvement that WRF outputs offer for drought analysis in this region with respect their driving data (ERA-Interim data), quantifying the added value of the dynamical downscaling to detect, monitor, and analyze drought events. For this, the drought indices were calculated by using the temperature and precipitation fields from the WRF model outputs (WRFERA), previously calibrated for the study region and compared with the ones computed from the observed data sets (mprmt). To analyze the added value provided by WRF, we also calculated the same drought indices by using their driving data (ERA).

The drought indices chosen were the SPI and SPEI, which are widely used indices due to their multiscalar character. The comparison between indices (SPEI or SPI), time scales (3 and 12 months), and source data for the computing of indices (mprmt, ERA, and WRFERA) was performed first by using a regionalization technique that provides a climatological classification in order to facilitate the interpretation of the results at regional scale and second by directly grid point to grid point, in order to analyze the added value provided by WRF for the local study of droughts.

The results indicate that simulations from WRF that generally capture reasonably well the drought temporal evolutions in all regions studied show reliable temporal correlations. These results are consistent with previous studies which found that different RCMs performed adequately drought characteristics in terms of drought indices such as the SPEI and the SPI [*Barrera-Escoda et al.*, 2014; *Maule et al.*, 2013] over different areas in Spain. Furthermore, we found that the results obtained by using downscaled fields outperform those

21698996, 2017, 3, Downloaded from https://agupubs.onlinelibrary.wiley.com/doi/10.1002/2016JD025683 by Readcube (Labtiva Inc.), Wiley Online Library on [27/01/2024]. See the Terms and Conditions (https://onlinelibrary.wiley.com/terms-and-conditions) on Wiley Online Library for rules of use; OA articles are governed by the applicable Creative Commons License

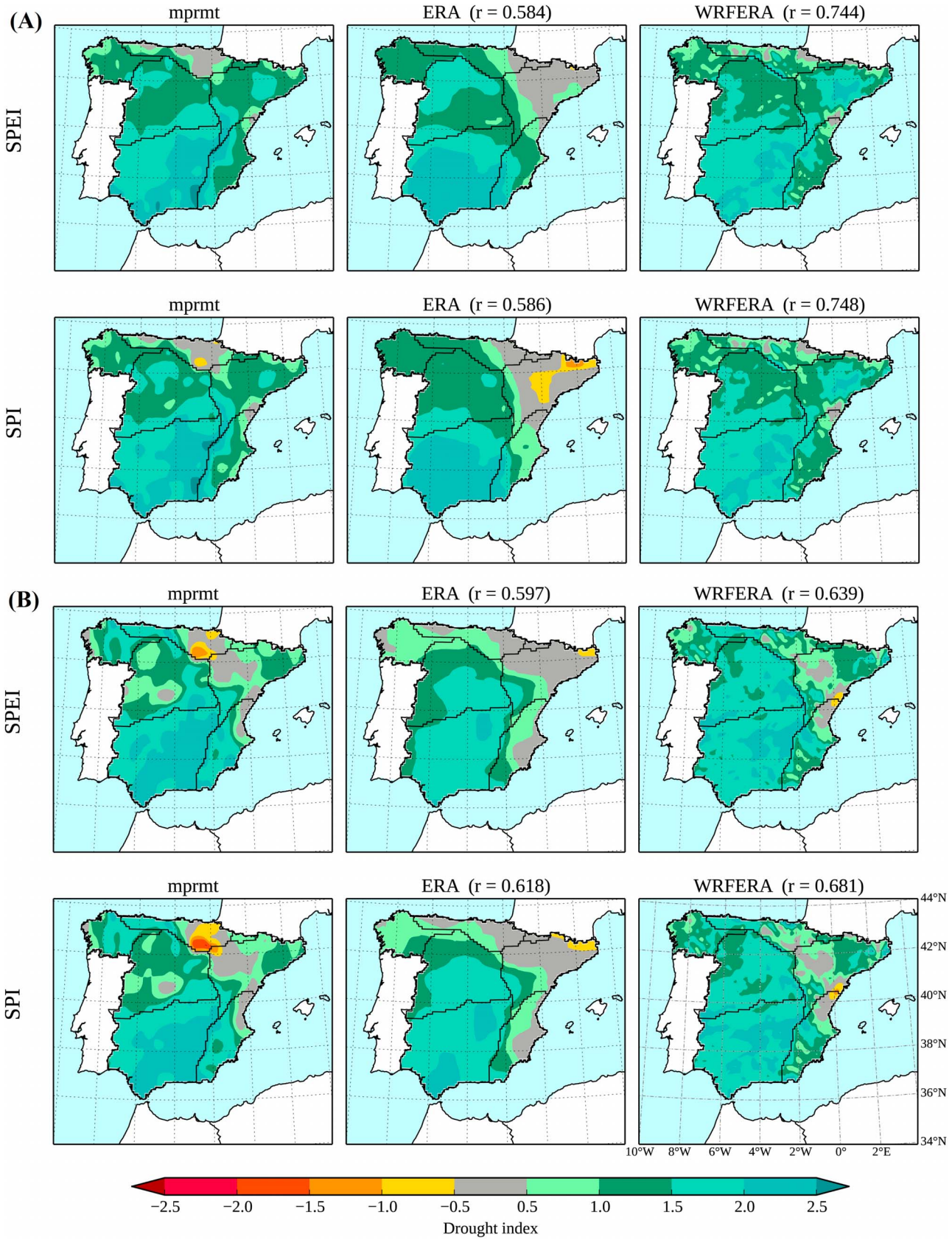

Figure 14. As in Figure 12 but for drought indices ending in (a) March 2010 and (b) November 2010.

21698996, 2017, 3, Downloaded from https://agupubs.onlinelibrary.wiley.com/doi/10.1002/2016JD025683 by Readcube (Labtiva Inc.), Wiley Online Library on [27/01/2024]. See the Terms and Conditions (https://onlinelibrary.wiley.com/terms-and-conditions) on Wiley Online Library for rules of use; OA articles are governed by the applicable Creative Commons License

21698996, 2017, 3, Downloaded from https://agupubs.onlinelibrary.wiley.com/doi/10.1002/2016JD025683 by Readcube (Labtiva Inc.), Wiley Online Library on [27/01/2024]. See the Terms and Conditions (https://onlinelibrary.wiley.com/terms-and-conditions) on Wiley Online Library for rules of use; OA articles are governed by the applicable Creative Commons License

from the driving data in terms of drought indices, the improvement being higher for the SPI than for the SPEI. This means that the dynamical downscaling could provide more reliable climate projections when assessing future drought episodes in a topographically complex area of terrain such as Spain. At a regional scale, the added value offered by WRF is strongly influenced by the time scale used, this being higher at longer time scales. Therefore, the results suggest that WRF outputs seem to be more appropriate than the driving data fields to monitor drought events in a context of water resources. These results agree with the findings of *Bowden et al.* [2016], who assessed the improvements provided for dynamical downscaling over the United States in a context of the SPI index.

Concerning the detailed study performed comparing grid points, the results from the analysis of the RMSE and the CSI agree with those from the regional study. These parameters broadly showed the improvements achieved by using WRF, and the influence of the time scale, with better results at 12 month time scale. The RMSE analysis showed worse agreement of drought indices simulated with respect to the mprmt in the northeastern and southeastern regions but better agreement in the southern and interior regions. These results are also in accordance with the regional study. The strongest improvements provided by WRF are for the regions that presented the worst results from ERA. By contrast, the CSI analysis also showed some areas where WRF did not provide any added improvement, so this behavior suggests that the ERA fields already resolved well in terms of drought events in some areas.

Regarding the study of duration, magnitude, and severity of individual drought periods, drought indices computed from ERA and WRFERA show difficulties to capture these drought characteristics, with worse agreement at 12 month time scale, as is reflected by the high spatial RMSE values in most of these parameters and for the Perkins SS. These results partially agree with the work of *PaiMazumder and Done* [2014] and *PaiMazumder et al.* [2013], who found that an ensemble of the Canadian Regional Climate Model presented problems in capturing the severity, frequency, and duration of drought events over Canada by using different drought indices. Our results for Spain also show that the added value of using WRF depended heavily on the time scale used, being clearer at 12 month time scale. At this time scale, the study of the relative differences from Perkins SS reveals that there is a significant improvement for magnitude and duration on average, while for intensity, the improvement is in terms of area extent.

The results of the analysis of the simulation of two particular extremely dry and wet events (winters of 2005 and 2009/2010) also suggest that WRF again provides an added value for the evaluation of extreme events, both for wet and dry periods, for most of Spain.

Finally, this study has also demonstrated that there is no substantial difference between the two drought indices, the SPEI and SPI, when evaluating the ability of WRF to simulate droughts in Spain. Although the improvement provided by WRF with respect to ERA data is higher for the SPI than for the SPEI simulations, the SPEI seems, in general, to provide slightly better results to detect wet and dry periods.

In summary, the results of this study show the benefit of using the WRF model to simulate downscaled fields for drought studies in the peninsular Spain, emphasizing the importance of the valuable information gathered at a local spatial scale, particularly relevant for drought-related decision making. The findings presented here provide valuable information about the validation of using the WRF model for further studies on drought projections in a climate change context.

Acknowledgments

This study has been financed by the Spanish Ministry of Economy and Competitiveness, with additional support from the European Community funds (FEDER), project CGL2013-48539-R, and the Regional Government of Andalusia, project P11-RNM-7941. We thank anonymous reviewers for valuable comments on the manuscript. We would also like to thank the ALHAMBRA supercomputer infrastructure (at the University of Granada) for providing us computer resources to carry out the work (https://alhambra.ugr.es). The authors thank José Carlos González-Hidalgo for providing the observational MOPREDAS and MOTEDAS data sets. The ERA-Interim data set was obtained from ECMWF (http://apps.ecmwf.int/datasets/data/interim-full-daily/levtype=sfc/) and the WRF model from NCAR (http://www.wrf-model.org/users/users.php). The drought indices computed by using WRF are available on a request to the authors (mgvaldecasas@ugr.es).

References

Allen, R. G., L. S. Pereira, D. Raes, and M. Smith (1998), *Crop Evapotranspiration: Guidelines for Computing Crop Water Requirements*, *FAO Irrig. and Drain. Pap.*, vol. 56, Food and Agric. Organ., Rome.

Argüeso, D., J. M. Hidalgo-Muñoz, S. R. Gámiz-Fortis, M. J. Esteban-Parra, J. Dudhia, and Y. Castro-Díez (2011), Evaluation of WRF parameterizations for climate studies over southern Spain using a multistep regionalization, *J. Clim.*, *24*, 5633–5651, doi:10.1175/JCLI-D-11-00073.1.

Argüeso, D., J. M. Hidalgo-Muñoz, S. R. Gámiz-Fortis, M. J. Esteban-Parra, and Y. Castro-Díez (2012a), Evaluation of WRF mean and extreme precipitation over Spain: Present climate (1970–99), *J. Clim.*, *25*, 4883–4897, doi:10.1175/JCLI-D-11-00276.1.

Argüeso, D., J. M. Hidalgo-Muñoz, S. R. Gámiz-Fortis, M. J. Esteban-Parra, and Y. Castro-Díez (2012b), High-resolution projections of mean and extreme precipitation over Spain using the WRF model (2070–2099 versus 1970–1999), *J. Geophys. Res.*, *117*, D12108, doi:10.1029/2011JD017399.

Barrera-Escoda, A., M. Gonçalves, D. Guerreiro, J. Cunillera, and J. M. Baldasano (2014), Projections of temperature and precipitation extremes in the North Western Mediterranean Basin by dynamical downscaling of climate scenarios at high resolution (1971–2050), *Clim. Change*, *122*, 567–582, doi:10.1007/s10584-013-1027-6.

Beguería, S., and S. M. Vicente-Serrano (2013), SPEI: Calculation of Standardized Precipitation-Evapotranspiration Index, R package version 1.6. [Available at http://cran.r-project.org/package=SPEI.]

Beguería, S., S. M. Vicente-Serrano, F. Reig, and B. Latorre (2014), Standardized Precipitation Evapotranspiration Index (SPEI) revisited: Parameter fitting, evapotranspiration models, tools, datasets and drought monitoring, *Int. J. Climatol.*, *34*, 3001–3023, doi:10.1002/joc.3887.

Berrisford, P., P. Kållberg, S. Kobayashi, D. Dee, S. Uppala, A. J. Simmons, P. Poli, and H. Sato (2011), Atmospheric conservation properties in ERA-Interim, *Q. J. R. Meteorol. Soc.*, *137*, 1381–1399, doi:10.1002/qj.864.

Betts, A. K., and M. J. Miller (1986), A new convective adjustment scheme. Part II: Single column tests using GATE wave, BOMEX, ATEX and arctic air-mass data sets, *Q. J. R. Meteorol. Soc.*, *112*, 693–709, doi:10.1002/qj.49711247308.

Blenkinsop, S., and H. J. Fowler (2007), Changes in European drought characteristics projected by the PRUDENCE regional climate models, *Int. J. Climatol.*, *27*, 1595–1610, doi:10.1002/joc.1538.

Boulard, D., T. Castel, P. Camberlin, A. S. Sergent, N. Bréda, V. Badeau, A. Rossi, and B. Pohl (2016), Capability of a regional climate model to simulate climate variables requested for water balance computation: A case study over northeastern France, *Clim. Dyn.*, *46*, 2689–2716, doi:10.1007/s00382-015-2724-9.

Bowden, J. H., K. D. Talgo, T. L. Spero, and C. G. Nolte (2016), Assessing the added value of dynamical downscaling using the Standardized Precipitation Index, *Adv. Meteorol.*, *2016*, 8432064, doi:10.1155/2016/8432064.

Burke, E. J., S. J. Brown, and N. Christidis (2006), Modeling the recent evolution of global drought for the twenty-first century with the Hadley Centre climate model, *J. Hydrometeorol.*, *7*, 1113–1125, doi:10.1175/JHM544.1.

Calinski, T., and J. Harabasz (1974), A dendrite method for cluster analysis, *Commun. Stat.*, *3*, 1–27, doi:10.1080/03610927408827101.

Chen, F., and J. Dudhia (2001), Coupling an advanced land surface-hydrology model with the Penn State-NCAR MM5 modeling system. Part I: Model implementation and sensitivity, *Mon. Weather Rev.*, *129*, 569–585, doi:10.1175/15200493(2001)129<0569:CAALSH > 2.0.CO;2.

Christensen, J. H., T. R. Carter, M. Rummukainen, and G. Amanatidis (2007), Evaluating the performance and utility of regional climate models: The PRUDENCE project, *Clim. Change*, *81*, 1–6, doi:10.1007/s10584-006-9211-6.

Collins, W. D., et al. (2004), Description of the NCAR Community Atmosphere Model (CAM 3.0), NCAR Tech. Note NCAR/TN-464+STR, doi:10.5065/D63N21CH.

Dee, D. P., et al. (2011), The ERA-Interim reanalysis: Configuration and performance of the data assimilation system, *Q. J. R. Meteorol. Soc.*, *137*, 553–597, doi:10.1002/qj.828.

Droogers, P., and R. G. Allen (2002), Estimating reference evapotranspiration under inaccurate data conditions, *Irrig. Drain. Syst.*, *16*, 33–45, doi:10.1023/A:1015508322413..

Fita, L., J. Fernández, and M. García-Díez (2010), CLWRF: WRF modifications for regional climate simulation under future scenarios, paper presented at 11th WRF Users' Workshop, NCAR, Boulder, Colo.

Fovell, R. G. (1997), Consensus clustering of U.S. temperature and precipitation data, *J. Clim.*, *10*, 1405–1427, doi:10.1175/1520-0442(1997)010<1405:CCOUST>2.0.CO;2.

García-Herrera, R., E. Hernández, D. Barriopedro, D. Paredes, R. M. Trigo, I. F. Trigo, and M. A. Mendes (2007), The outstanding 2004/05 drought in the Iberian Peninsula: Associated atmospheric circulation, *J. Hydrometeorol.*, *8*, 483–498, doi:10.1175/JHM578.1.

García-Valdecasas-Ojeda, M., S. R. Gámiz-Fortis, J. M. Hidalgo-Muñoz, D. Argüeso, Y. Castro-Díez, and M. J. Esteban-Parra (2015), Regional climate model sensitivity to different parameterizations schemes with WRF over Spain, paper presented at EGU General Assembly 2015, EGU, Vienna, Au., 12–17 Apr.

Giorgi, F., C. Jones, and G. R. Asrar (2009), Addressing climate information needs at the regional level: The CORDEX framework, *WMO Bull.*, *58*(3), 175–183.

Gonçalves, M., A. Barrera-Escoda, D. Guerreiro, J. M. Baldasano, and J. Cunillera (2014), Seasonal to yearly assessment of temperature and precipitation trends in the North Western Mediterranean Basin by dynamical downscaling of climate scenarios at high resolution (1971–2050), *Clim. Change*, *122*, 243–256, doi:10.1007/s10584-013-0994-y.

González-Hidalgo, J. C., M. Brunetti, and M. de Luis (2011), A new tool for monthly precipitation analysis in Spain: MOPREDAS database (monthly precipitation trends December 1945–November 2005), *Int. J. Climatol.*, *31*, 715–731, doi:10.1002/joc.2115.

González-Hidalgo, J. C., D. Peña-Angulo, M. Brunetti, and N. Cortesi (2015), MOTEDAS: A new monthly temperature database for mainland Spain and the trend in temperature (1951–2010), *Int. J. Climatol.*, *35*, 4444–4463, doi:10.1002/joc.4298.

Guttman, N. B. (1998), Comparing the Palmer drought index and the Standardized Precipitation Index, *J. Am. Water Resour. Assoc.*, *34*, 113–121, doi:10.1111/j.1752-1688.1998.tb05964.x.

Hamdi, R., H. Van de Vyver, R. De Troch, and P. Termonia (2014), Assessment of three dynamical urban climate downscaling methods: Brussels's future urban heat island under an A1B emission scenario, *Int. J. Climatol.*, *34*, 978–999, doi:10.1002/joc.3734.

Heikkilä, U., A. Sandvik, and A. Sorteberg (2011), Dynamical downscaling of ERA-40 in complex terrain using the WRF regional climate model, *Clim. Dyn.*, *37*, 1551–1564, doi:10.1007/s00382-010-0928-6.

Hong, S. Y., J. Dudhia, and S. Chen (2004), A revised approach to ice microphysical processes for the bulk parameterization of clouds and precipitation, *Mon. Weather Rev.*, *132*, 103–120, doi:10.1175/1520-0493(2004)132<0103:ARATIM>2.0.CO;2.

Jacob, D., et al. (2014), EURO-CORDEX: New high-resolution climate change projections for European impact research, *Reg. Environ. Change*, *14*, 563–578, doi:10.1007/s10113-013-0499-2.

Janjic, Z. I. (1990), The step-mountain coordinate: Physical package, *Mon. Weather Rev.*, *118*, 1429–1443, doi:10.1175/1520-0493(1990)118<1429:TSMCPP>2.0.CO;2.

Janjic, Z. I. (1994), The step-mountain eta coordinate model: Further developments of the convection, viscous sublayer, and turbulence closure schemes, *Mon. Weather Rev.*, *122*, 927–945, doi:10.1175/1520-0493(1994)122<0927:TSMECM>2.0.CO;2.

Kala, J., J. Andrys, T. J. Lyons, I. J. Foster, and B. J. Evans (2015), Sensitivity of WRF to driving data and physics options on a seasonal time-scale for the southwest of Western Australia, *Clim. Dyn.*, *44*, 633–659, doi:10.1007/s00382-014-2160-2.

Kang, D., B. K. Eder, A. F. Stein, G. A. Grell, S. E. Peckham, and J. McHenry (2005), The New England air quality forecasting pilot program: Development of an evaluation protocol and performance benchmark, *J. Air Waste Manage.*, *55*, 1782–1796, doi:10.1080/10473289.2005.10464775.

Kennedy, J., D. Parker, and H. Coleman (2006), Global and regional climate in 2005, *Weather*, *61*(8), 215–224, doi:10.1256/wea.72.06.

Kim, B. S., I. G. Chang, J. H. Sung, and H. J. Han (2016), Projection in future drought hazard of South Korea based on RCP climate change scenario 8.5 using SPEI, *Adv. Meteorol.*, *2016*, 4148710, doi:10.1155/2016/4148710.

Lindner, M., et al. (2010), Climate change impacts, adaptive capacity, and vulnerability of European forest ecosystems, *For. Ecol. Manag.*, *259*, 698–709, doi:10.1016/j.foreco.2009.09.023.

Maule, C. F., P. Thejll, J. H. Christensen, S. H. Svendsen, and J. Hannaford (2013), Improved confidence in regional climate model simulations of precipitation evaluated using drought statistics from the ENSEMBLES models, *Clim. Dyn.*, *40*, 155–173, doi:10.1007/s00382-012-1355-7.

McKee, T. B., N. J. Doesken, and J. Kleist (1993), The relationship of drought frequency and duration to time scales, paper presented at 8th Conference on Applied Climatology, Am. Meteorol. Soc., Anaheim, California, 17–22 Jan.

21698996, 2017, 3, Downloaded from https://agupubs.onlinelibrary.wiley.com/doi/10.1002/2016JD025683 by Readcube (Labtiva Inc.), Wiley Online Library on [27/01/2024]. See the Terms and Conditions (https://onlinelibrary.wiley.com/terms-and-conditions) on Wiley Online Library for rules of use; OA articles are governed by the applicable Creative Commons License

Meque, A., and B. J. Abiodun (2015), Simulating the link between ENSO and summer drought in Southern Africa using regional climate models, *Clim. Dyn.*, *44*, 1881–1900, doi:10.1007/s00382-014-2143-3.
Miguez-Macho, G., G. L. Stenchikov, and A. Robock (2004), Spectral nudging to eliminate the effects of domain position and geometry in regional climate model simulations, *J. Geophys. Res.*, *109*, D13104, doi:10.1029/2003JD004495.
Mishra, A. K., and V. P. Singh (2010), A review of drought concepts, *J. Hydrol.*, *391*, 202–216, doi:10.1016/j.jhydrol.2010.07.012.
PaiMazumder, D., and J. M. Done (2014), Uncertainties in long-term drought characteristics over the Canadian Prairie Provinces, as simulated by the Canadian RCM, *Clim. Res.*, *58*, 209–220, doi:10.3354/cr01196.
PaiMazumder, D., L. Sushama, R. Laprise, M. N. Khaliq, and D. Sauchyn (2013), Canadian RCM projected changes to short- and long-term drought characteristics over the Canadian Prairies, *Int. J. Climatol.*, *33*, 1409–1423, doi:10.1002/joc.3521.
Palmer, W. C. (1965), *Meteorological Drought*, *Res. Pap.*, vol. 45, pp. 58, U.S. Dep. of Commerce, Washington, D. C.
Pan, Z., E. Takle, W. Gutowski, and R. Turner (1999), Long simulation of regional climate as a sequence of short segments, *Mon. Weather Rev.*, *127*, 308–321, doi:10.1175/1520-0493(1999)127<0308:LSORCA>2.0.CO;2.
Pérez, J. C., J. P. Díaz, A. González, J. Expósito, F. Rivera-López, and D. Taima (2014), Evaluation of WRF parameterizations for dynamical downscaling in the Canary Islands, *J. Clim.*, *27*, 5611–5631, doi:10.1175/JCLI-D-13-00458.1.
Perkins, S. E., A. J. Pitman, N. J. Holbrook, and J. McAneney (2007), Evaluation of the AR4 climate models' simulated daily maximum temperature, minimum temperature, and precipitation over Australia using probability density functions, *J. Clim.*, *20*, 4356–4376, doi:10.1175/2FJCLI4253.1.
Pleim, J. E. (2007), A combined local and nonlocal closure model for the atmospheric boundary layer. Part I: Model description and testing, *J. Appl. Meteorol. Climatol.*, *46*, 1396–1409, doi:10.1175/JAM2539.1.
Richman, M. B. (1986), Rotation of principal components, *J. Clim.*, *6*, 293–335, doi:10.1002/joc.3370060305.
Russo, A. C., C. M. Gouveia, R. M. Trigo, L. R. M. L. R. Liberato, and C. C. DaCamara (2015), The influence of circulation weather patterns at different spatial scales on drought variability in the Iberian Peninsula, *Front. Environ. Sci.*, *3*, 1–15, doi:10.3389/fenvs.2015.00001.
Sánchez, E., M. Domínguez, R. Romera, N. López de la Franca, M. A. Gaertner, C. Gallardo, and M. Castro (2011), Regional modeling of dry spells over the Iberian Peninsula for present climate and climate change conditions, *Clim. Change*, *107*, 625–634, doi:10.1007/s10584-011-0114-9.
Santos, J. F., I. Pulido-Calvo, and M. M. Portela (2010), Spatial and temporal variability of droughts in Portugal, *Water Resour. Res.*, *46* W03503, doi:10.1029/2009WR008071.
Sheffield, J., and E. F. Wood (2008), Projected changes in drought occurrence under future global warming from multi-model, multi-scenario, IPCC AR4 simulations, *Clim. Dyn.*, *31*, 79–105, doi:10.1007/s00382-007-0340-z.
Sims, A. P., D. S. Nigoyi, and S. Raman (2002), Adopting indices for estimating soil moisture: A North Carolina case study, *Geophys. Res. Lett.*, *29*(8), 1183, doi:10.1029/2001GL013343.
Skamarock, W. C., J. B. Klemp, J. Dudhia, D. O. Gill, D. M. Barker, M. G. Duda, X. Y. Huang, W. Wang, and J. G. Powers (2008), A description of the advanced research WRF version 3, 125 pp., NCAR Tech. Note NCAR/TN-475 + STR, doi:10.5065/D68S4MVH.
Vicente-Serrano, S. M. (2006), Differences in spatial patterns of drought on different time scales: An analysis of the Iberian Peninsula, *Water Resour. Manage.*, *20*, 37–60, doi:10.1007/s11269-006-2974-8.
Vicente-Serrano, S. M., J. C. González-Hidalgo, M. de Luis, and J. Reventós (2004), Drought patterns in the Mediterranean area: The Valencia region (eastern Spain), *Clim. Res.*, *26*, 5–15, doi:10.3354/cr026005.
Vicente-Serrano, S. M., S. Beguería, and J. I. López-Moreno (2010), A multiscalar drought index sensitive to global warming: The Standardized Precipitation Evapotranspiration Index, *J. Clim.*, *23*, 1696–1718, doi:10.1175/2009JCLI29091.
Vicente-Serrano, S. M., J. I. López-Moreno, A. Drumond, L. Gimeno, R. Nieto, E. Morán-Tejeda, J. Lorenzo-Lacruz, S. Beguería, and J. Zabalza (2011a), Effects of warming processes on droughts and water resources in the NW Iberian Peninsula (1930–2006), *Clim. Res.*, *48*, 203–212, doi:10.3354/cr01002.
Vicente-Serrano, S. M., R. M. Trigo, J. I. López-Moreno, M. L. R. Liberato, J. Lorenzo-Lacruz, S. Beguería, E. Morán-Tejeda, and A. El Kanawi (2011b), Extreme winter precipitation in the Iberian Peninsula in 2010: Anomalies, driving mechanisms and future projections, *Clim. Res.*, *46*, 51–65, doi:10.3354/cr00977.
Vicente-Serrano, S. M., S. Beguería, and J. I. López-Moreno (2011c), Comment on "Characteristics and trends in various forms of the Palmer Drought Severity Index (PDSI) during 1900–2008" by Aiguo Dai, *J. Geophys. Res.*, *116*, D19112, doi:10.1029/2011JD016410.
Vicente-Serrano, S. M., C. Azorin-Molina, A. Sánchez-Lorenzo, J. Revuelto, E. Morán-Tejeda, J. I. López-Moreno, and F. Espejo (2014a), Sensitivity of reference evapotranspiration to changes in meteorological parameters in Spain (1961–2011), *Water Resour. Res.*, *50*, 8458–8480, doi:10.1002/2014WR015427.
Vicente-Serrano, S. M., et al. (2014b), Evidence of increasing drought severity caused by temperature rise in southern Europe, *Environ. Res. Lett.*, *9*, doi:10.1088/1748-9326/9/4/044001.
von Storch, H., H. Langenberg, and F. Feser (2000), A spectral nudging technique for dynamical downscaling purposes, *Mon. Weather Rev.*, *128*, 3664–3673, doi:10.1175/1520-0493(2000)128<3664:ASNTFD>2.0.CO;2.
Waldron, K. M., J. Paegle, and J. D. Horel (1996), Sensitivity of a spectrally filtered and nudged limited area model to outer model options, *Mon. Weather Rev.*, *124*, 529–547, doi:10.1175/1520-0493(1996)124<0529:SOASFA>2.0.CO;2.
Wang, G. (2005), Agricultural drought in a future climate: Results from 15 global climate models participating in the IPCC 4th assessment, *Clim. Dyn.*, *25*, 739–753, doi:10.1007/s00382-005-0057-9.
Wang, J., F. N. U. Swati, M. L. Stein, and V. R. Kotamarthi (2015), Model performance in spatiotemporal patterns of precipitation: New methods for identifying value added by a regional climate model, *J. Geophys. Res. Atmos.*, *120*, 1239–1259, doi:10.1002/2014JD022434.
Wang, W., M. W. Ertsen, M. D. Svoboda, and M. Hafeez (2016), Propagation of drought: From meteorological drought to agricultural and hydrological drought, *Adv. Meteorol.*, *2016*, 6547209, doi:10.1155/2016/6547209.
Wilks, D. S. (2006), *Statistical Methods in the Atmospheric Sciences, International Geophysics Series*, vol. 91, Academic Press, Burlington, Mass.
Yang, Y., H. Kuo, E. A. Hendricks, Y. Liu, and M. S. Peng (2015), Relationship between typhoons with concentric eyewalls and ENSO in the western North Pacific basin, *J. Clim.*, *28*, 3612–3623, doi:10.1175/JCLI-D-14-00541.1.
Yu, M., Q. Li, M. J. Hayes, M. D. Svoboda, and R. R. Heim (2014), Are droughts becoming more frequent or severe in China based on the Standardized Precipitation Evapotranspiration Index: 1951–2010?, *Int. J. Climatol.*, *34*, 545–558, doi:10.1002/joc.3701.

21698996, 2017, 3, Downloaded from https://agupubs.onlinelibrary.wiley.com/doi/10.1002/2016JD025683 by Readcube (Labtiva Inc.), Wiley Online Library on [27/01/2024]. See the Terms and Conditions (https://onlinelibrary.wiley.com/terms-and-conditions) on Wiley Online Library for rules of use; OA articles are governed by the applicable Creative Commons License